International Journal of Control
Vol. 00, No. 00, DD Month 200x, 1–26

Non-local Stabilization of a Spherical Inverted Pendulum

Guangyu Liu, Dragan Nešić, and Iven Mareels*

Department of Electrical & Electronic Engineering,
The University of Melbourne, Parkville, 3010, Victoria, Australia.

(*v1.1 released January 2006*)

We design a nonlinear stabilizing control law for a four degree of freedom spherical inverted pendulum. The pendulum is a slim cylindrical beam attached to a horizontal plane via a universal joint; the joint is free to move in the plane under the influence of a planar force. The upright position is an unstable equilibrium of the uncontrolled system because of gravity. The objective is to design a controller so that it stabilizes the upright position starting from any position in the upper hemisphere with arbitrary velocity. We achieve this by first transforming the original system to an appropriate upper triangular form and then designing a controller which incorporates a high gain design with the method of nonlinear forwarding. The control law is evaluated through computer simulations.

Key words: a spherical inverted pendulum, forwarding, nested saturation, nonlinear

1 Introduction

The spherical inverted pendulum is a slim cylindrical beam attached to a horizontal plane via a universal joint (see Figure 1). The universal joint is free to move in the plane, under the influence of a planar force – the control signal. Because of the gravity force, the downward and upward positions are respectively the stable equilibrium and the unstable equilibrium of the uncontrolled system. The control objective considered here is to use the planar force to drive the inverted pendulum in such a way that the upright position is asymptotically stable and attractive from any starting position in the upper hemisphere with arbitrary initial velocities. Moreover, the pendulum's universal joint has to be returned to a given point on the plane and remain there. We do not consider the problem of swing up of the pendulum and rather assume that initial conditions are located in the upper hemisphere.

The spherical inverted pendulum is commonly found in control laboratories. Its model resembles several other systems found in robotics and aerospace engineering. For instance, the spherical inverted pendulum is an abstraction for a vector thrust controlled body hovering at a given altitude.

The control of a spherical inverted pendulum is considered in Albouy and Praly (2000); Yang *et al.* (2000); Chung *et al.* (2000); Bloch *et al.* (2000, 2001); Angeli (2001a). In Albouy and Praly (2000), a swing-up strategy is proposed based on passivity. Stabilizing the pendulum locally around an operating point is discussed in Yang *et al.* (2000); Chung *et al.* (2000), where the pendulum is analyzed under the assumption of small deviations from the vertical upright position. Two continuous controllers in the literature attempt to achieve nonlocal stabilization of the pendulum Bloch *et al.* (2000, 2001); Angeli (2001a). In Bloch *et al.* (2000, 2001), the authors use the controlled Lagrangian framework to derive a controller to regulate the angles for a spherical pendulum. In Angeli (2001a), a control idea is proposed for the pendulum based on the regulation of the velocity of the nutation angle and then it is pointed out that the problem of controlling the spherical inverted pendulum maybe reduced to the problem of a planar inverted pendulum allowing the results for the planar inverted pendulum in Angeli (2001b) and Teel (1996)

*Corresponding author. Email: {g.liu, d.nesic, i.mareels}@ee.unimelb.edu.au

International Journal of Control
ISSN 0020-7179 print/ ISSN 1366-5820 online ©2005 Taylor & Francis Ltd
http://www.tandf.co.uk/journals
DOI: 10.1080/00207170xxxxxxxxxxxx

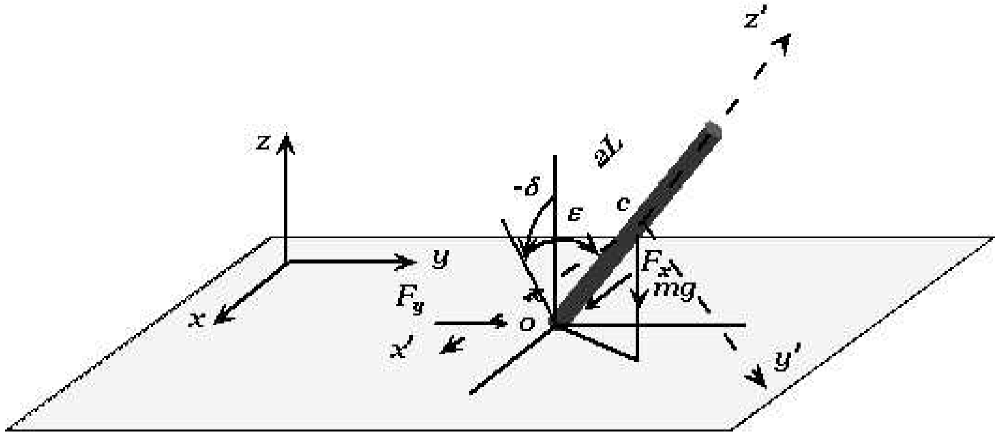

Figure 1. The spherical inverted pendulum

to be applied. However, to the best of our knowledge, no complete solution for the stabilization/regulation of all four degrees of freedom of a spherical inverted pendulum has appeared in the literature.

In this paper, we develop a nonlinear controller that stabilizes the upright position of the pendulum such that the upper hemisphere is its domain of attraction. The controller design consists of several steps. In the first step, we take a state transformation and a control transformation to convert the system to a globally defined system in the upper triangular form. Next, we design a controller for a subsystem that will be a starting point in a forwarding controller design. Finally, we use the forwarding method proposed in Teel (1996) to construct a controller for the overall system. Our design relies on results and ideas from Teel (1996) and Angeli (2001a).

The full model of the spherical pendulum is highly nonlinear. Since the self-spin around the symmetry axis of the slim cylindrical beam is ignored and the universal joint of the pendulum is restricted by the horizontal plane, the spherical pendulum has four degrees of freedom. We work with the position of the universal joint in the plane (x, y) and the pitch and roll angles (δ, ϵ) of the beam (see Figure 1). The proposed controller brings the pendulum from any initial condition in the upper hemisphere to the upright position. The set of coordinates is suggested in Olfati-Saber (2001) for a simplified spherical inverted pendulum on the cart where the mass of the pendulum concentrates on a bob. We consider here a slightly more general case–a slim cylindrical beam with the uniform mass density where the rotational kinetic energy about the centre of mass is taken into account[1]. A low and high gain controller based on the same idea is also designed for an alternative set of coordinates in the conference version of this paper Liu *et al.* (2005).

The paper is organized as follows. We recall some results from nonlinear control theory in Section II. In Section III, we derive the model in a form that will allow us to use the forwarding method. Then, we complete the control design in Section IV and present some simulations in Section V. Final observations are given in Section VI.

---

[1]The rotational kinetic energy about the symmetry axis of the slim cylindrical beam is ignored considering that the radius of the slim beam is much less than its length.

2 Preliminaries

2.1 *Notations*

Class $\mathcal{K}$ function: a continuous function $\alpha : [0, a) \to [0, \infty)$ is said to belong to class $\mathcal{K}$ if it is strictly increasing and $\alpha(0) = 0$.

Class $\mathcal{K}_\infty$ function: If $a = \infty$ and $\lim_{r\to\infty} \alpha(r) = \infty$, the function is said to belong to class $\mathcal{K}_\infty$.

Class $\mathcal{KL}$ function: a continuous function $\beta(s, t) : [0, a) \times [0, \infty) \to [0, \infty)$ is said to belong to class $\mathcal{KL}$ if, for each fixed t, the function β belongs to class $\mathcal{K}$ and, for each fixed s, the function β is decreasing and $\lim_{s\to\infty} \beta(s, 0) = 0$.

For a piecewise-continuous function $u : [0, \infty) \to R^m$, define $\|u(\cdot)\|_a = \limsup_{t\to\infty}\{\max_{1\le i\le m} |u_i(t)|\}$. The quantity thus introduced is referred to as the asymptotic "norm" of $u(\cdot)$.

Asymptotic gain Teel (1996); Isidori (1999): System $\dot{x} = f(x, u)$, $y = h(x, u)$ is said to satisfy an asymptotic (input-output) bound, with restriction X on $x(0)$ and restriction U on $u(\cdot)$, if there exists a class $\mathcal{K}$ function $\gamma_u(\cdot)$, called the gain function, such that, for any $x(0) \in X$ and for any piecewise-continuous input $u(\cdot)$ satisfying $\|u(\cdot)\|_a < U$, the response $x(t)$ for the initial state $x(0)$ exists for all $t \ge 0$ and is such that $\|y(\cdot)\|_a \le \gamma_u(\|u(\cdot)\|_a)$.

For a vector $x \in R^n$, $\|x\| = (|x_1|^2 + \ldots + |x_n|^2)^{1/2}$ denotes the Euclidean norm. Let $u(t) : [0, \infty) \to R^m$ be any piecewise continuous bounded function. The set of all such functions, endowed with the supremum norm $\|u(\cdot)\|_\infty = \sup_{t\ge0} \|u(t)\|$, is denoted by L^m_∞.

We use $(x_1, x_2) \triangleq (x_1^T, x_2^T)^T$ for convenience. A saturation function is $\sigma(s) \triangleq \begin{cases} sgn(s), & |s| > 1 \\ s, & |s| \le 1 \end{cases}$ where sgn is the sign function. C^- denotes the left hand side of the complex plane. $\mathbf{I}$ denotes the identity matrix.

2.2 *Input-output Feedback Linearization of MIMO System*

We recall the method of input-output feedback linearization for square MIMO systems (Slotine and Li, 1991, Ch.6). Consider the system

$$\dot{x} = f(x) + g(x)u, \quad y = h(x), \tag{1}$$

where $x \in R^n$ is the state vector, $u \in R^m$ is the control input, $y \in R^m$ the system output, f, h and g_i are smooth vector fields. Assume that r_i is the smallest integer such that at least one of the inputs appears in $\frac{d^{r_i} y_i}{dt^{r_i}}$ for the output y_i. This yields

$$\begin{aligned} \begin{pmatrix} \frac{d^{r_1} y_1}{dt^{r_1}} \\ \vdots \\ \frac{d^{r_m} y_m}{dt^{r_m}} \end{pmatrix} &= \begin{pmatrix} \mathcal{L}_f^{r_1} h_1(x) \\ \vdots \\ \mathcal{L}_f^{r_m} h_m(x) \end{pmatrix} + \begin{pmatrix} \sum_{j=1}^m \mathcal{L}_{g_j} \mathcal{L}_f^{r_1-1} h_j(x) u_j \\ \vdots \\ \sum_{j=1}^m \mathcal{L}_{g_j} \mathcal{L}_f^{r_m-1} h_j(x) u_j \end{pmatrix} \\ &\triangleq \mathcal{L}_f^r h(x) + E(x)u, \end{aligned} \tag{2}$$

where $\mathcal{L}_{g_j}\mathcal{L}_f^{r_i-1} h_j(x) \ne 0$, $i = 1, \ldots, m$ for at least one j, in a neighborhood χ_i of the point x_0. Then, the system (1) is said to have a vector relative degree $(r_1, \ldots, r_m)$ at x_0. Define χ as the intersection of the χ_i and assume $E(x)$ is invertible over the region χ. Then, the input transformation

$$u = E^{-1}(x)(v - \mathcal{L}_f^r h(x)), \tag{3}$$

yields m equations of the simple form

$$\frac{d^{r_i} y_i}{dt^{r_i}} = v_i\ , \tag{4}$$

that is, the system is input-output linearized.

2.3 *ISS and ISS-Lyapunov Function*

We review a key nonlinear analysis tool, input-to-state stability (ISS) and related results discussed by Sontag and coworkers in Sontag (1989, 1990); Sontag and Wang (1995). See also the monograph (Isidori, 1999, Chapter 10).

ISS : The system

$$\dot{x} = f(x, u) \tag{5}$$

is said to be ISS if there exist a class $\mathcal{KL}$ function $\beta(\cdot,\cdot)$ and a class $\mathcal{K}$ function $\gamma(\cdot)$, such that for any input $u(\cdot) \in L^m_\infty$ and any $x(0) \in R^n$, the response $x(t)$ satisfies $\|x(t)\| \leq \beta(\|x(0)\|, t) + \gamma(\|u(\cdot)\|_\infty)$.

ISS-Lyapunov function: A C^1 function V is called an ISS-Lyapunov funtion for system (5) if there exist class $\mathcal{K}_\infty$ functions $\underline{a}(\cdot)$, $\overline{a}(\cdot)$, $a(\cdot)$ and a class $\mathcal{K}$ function $\chi(\cdot)$ such that

$$\underline{a}(\|x\|) \leq V(x) \leq \overline{a}(\|x\|) \text{ for all } x \in R^n \tag{6}$$

and

$$\|x\| \geq \chi(\|u\|) \Rightarrow \frac{\partial V}{\partial x} f(x, u) \leq -a(\|x\|) \text{ for all } x \in R^n. \tag{7}$$

THEOREM 2.1 Sontag and Wang (1995) *System (5) is input-to-state stable if and only if there exists an ISS-Lyapunov function.*

2.4 *Nested Saturation Design to Forwarding Systems*

The next result is a key design tool in forwarding.

THEOREM 2.2 Teel (1996)(Isidori, 1999, Lemma 14.3.5) *Consider the system*

$$\dot{z} = Az + g_i(\xi_i, u), \quad \dot{\xi}_i = f_i(\xi_i, u) \tag{8}$$

in which $z \in \mathrm{R}^n$, $\xi_i \in \mathrm{R}^p$, $u \in \mathrm{R}^m$, $g_i(\xi_i, u)$ *and* $f_i(\xi_i, u)$ *are locally Lipschitz, differentiable at* $(\xi_i, u) = (0, 0)$*, and* $g_i(0, 0) = 0$, $f_i(0, 0) = 0$*. Assume that:*

(i) there exists a symmetric matrix $P > 0$ *such that* $PA + A^T P \leq 0$,

(ii) the linear approximation of the system at the equilibrium $(z_i, \xi_i, u) = (0, 0, 0)$ *is stabilizable.*

There exists a function $\alpha_i : R^v \times R^m \to R^m$ *(i.e.,* $(\xi_i, v) \mapsto \alpha_i(\xi_i, v)$*), with* $\alpha_i(0, 0) = 0$*, which is locally Lipschitz, differentiable at* $(\xi_i, v) = (0, 0)$*, with the following properties:*

(iiia) the matrix $\left[\frac{\partial \alpha_i(\xi_i,v)}{\partial v}\right]_{(0,0)}$ *is nonsingular,*

(iiib) the matrix $\left[\frac{\partial f_i(\xi_i,\alpha_i(\xi_i,v))}{\partial \xi_i}\right]_{(0,0)}$ *has all eigenvalues in* C^-,

(iiic) the system $\dot{\xi}_i = f_i(\xi_i, \alpha_i(\xi_i, v))$, $y = \xi_i$ *satisfies an asymptotic (input* v *to output* y *) bound , with restriction* X_i *on* ξ_i°*, restriction* $V > 0$ *on* $v(\cdot)$*, with linear gain function.*

Let $\xi_{i+1} = (z, \xi_i)$, $\tilde{v} = n + p$, $f_{i+1}(\xi_{i+1}, u) = \begin{pmatrix} Az + g_i(\xi_i, u) \\ f_i(\xi_i, u) \end{pmatrix}$, $F_{i+1} = \left[\frac{\partial f_{i+1}(\xi_{i+1},\alpha_i(\xi_i,v))}{\partial \xi_{i+1}}\right]_{(0,0)}$, $G_{i+1} = \left[\frac{\partial f_{i+1}(\xi_{i+1},\alpha_i(\xi_i,v))}{\partial v}\right]_{(0,0)}$.

Then, the pair (F_{i+1}, G_{i+1}) *is stabilisable.*

Let $\sigma(\cdot)$ *be any* R^m *-valued saturation function. Pick a* $\tilde{v} \times m$ *matrix* K_{i+1} *such that* $(F_{i+1} + G_{i+1}K_{i+1})$ *has all eigenvalues in* C^- *and, for some* $\delta' > 0$*, system* $\dot{x} = F_{i+1}x + G_{i+1}\sigma(K_{i+1}x + v) + w$, $y = x$ *satisfies an asymptotic (input (v,w) to output y) bound, with no restriction on* x° *and restriction* δ' *on* $v(\cdot)$ *and*

$w(\cdot)$, with linear gain functions $\gamma_v(\cdot)$ and $\gamma_w(\cdot)$. Pick two $m \times m$ matrices Γ and Ω such that $\Gamma + \Omega$ is nonsingular. Consider the function

$$\begin{array}{l} \alpha_{i+1} : R^{\tilde{v}} \times R^m \to R^m \\ (\xi_{i+1}, v) \mapsto \alpha_i \left(\xi_i, \lambda\sigma\left(\frac{K_{i+1}\xi_{i+1}+\Gamma v}{\lambda}\right) + \Omega v \right) \end{array} .$$

Then, there exist numbers $\lambda > 0$ and $\tilde{V} > 0$ such that

(a) the matrix $\left[\frac{\partial \alpha_{i+1}(\xi_{i+1},v)}{\partial v}\right]_{(0,0)}$ is nonsingular,

(b) the matrix $\left[\frac{\partial f_{i+1}(\xi_{i+1},\alpha_{i+1}(\xi_{i+1},v))}{\partial \xi_{i+1}}\right]_{(0,0)}$ has all eigenvalues in C^-,

(c) the system $\dot{\xi}_{i+1} = f_{i+1}(\xi_{i+1}, \alpha_{i+1}(\xi_{i+1}, v))$, $y = \xi_{i+1}$ satisfies an asymptotic (input v - output y) bound, with restriction $X_{i+1} = R^n \times X_i$ on ξ°_{i+1}, restriction $\tilde{V} > 0$ on $v(\cdot)$, with linear gain function.

This result can be repeatedly used to globally asymptotically stabilize a system in the so called forwarding form.

3 The Dynamic Model

In this section we derive a model for the spherical inverted pendulum using coordinates: the position of the universal joint in the plane (x, y), the pitch angle δ and the roll angle ϵ coordinates as indicated in Figure 1 where the pitch angle δ is the rotation around y-axis and the roll angle ϵ is the rotation around the body fixed frame x'-axis. Let $q \triangleq (x, y, \delta, \epsilon)$.

The kinetic energy and potential energy of the pendulum are calculated next. Two vectors are defined to indicate the positions of the pivot o and the center of mass c respectively

$$P_o = (x, y, 0)\,,\; P_c = (x - L\sin\delta, y + L\cos\delta\sin\epsilon, L\cos\delta\cos\epsilon).$$

Their time derivative gives the velocity vectors

$$\dot{P}_o = (\dot{x}, \dot{y}, 0)\,,\; \dot{P}_c = (\dot{x} - L\dot{\delta}\cos\delta, \dot{y} + L\dot{\epsilon}\cos\epsilon\cos\delta - L\dot{\delta}\sin\epsilon\sin\delta, -L\dot{\epsilon}\sin\epsilon\cos\delta - L\dot{\delta}\cos\epsilon\sin\delta).$$

The angular velocity ω of the inverted pendulum in the body fixed frame (x', y', z') with the origin at the centre of mass c can be expressed as [1]

$$\omega = (\omega_1, \omega_2, \omega_3) = (\dot{\epsilon}, \dot{\delta}\cos\epsilon, -\dot{\delta}\sin\epsilon), \tag{9}$$

and the principal moment of inertia tensor with respect to the body fixed frame is

$$I = \begin{pmatrix} I_1 & 0 & 0 \\ 0 & I_2 & 0 \\ 0 & 0 & I_3 \end{pmatrix} = \begin{pmatrix} \frac{L^2m}{3} + \frac{R^2m}{4} & 0 & 0 \\ 0 & \frac{L^2m}{3} + \frac{R^2m}{4} & 0 \\ 0 & 0 & \frac{R^2m}{2} \end{pmatrix}. \tag{10}$$

The kinetic energy of the pendulum consists of two terms: translational kinetic energy and rotational kinetic energy with respect to the center of mass

$$\begin{aligned} T &= \frac{1}{2}m\langle \dot{P}_c, \dot{P}_c\rangle + \frac{1}{2}\omega I \omega^T \\ &= \frac{1}{2}(\dot{x}, \dot{y}, \dot{\delta}, \dot{\epsilon})\mathbf{D}(q)(\dot{x}, \dot{y}, \dot{\delta}, \dot{\epsilon})^T, \end{aligned} \tag{11}$$

[1] This is obtained by taking the Euler angle transformation $2-1-3$: pitch δ, roll ϵ and yaw angle γ where $\gamma \equiv 0$ and its rate $\dot{\gamma} \equiv 0$ is assumed (i.e., self-spin about z' axis is ignored).

where $\mathbf{D}(q)$ is the inertia tensor (see Appendix A). The potential energy of the system is

$$V = mgL\cos\epsilon\cos\delta\,. \tag{12}$$

The Lagrangian is,

$$\mathcal{L} \triangleq \frac{1}{2}(\dot{x}, \dot{y}, \dot{\delta}, \dot{\epsilon})\mathbf{D}(q)(\dot{x}, \dot{y}, \dot{\delta}, \dot{\epsilon})^T - mgL\cos\delta\cos\epsilon\,. \tag{13}$$

The Euler-Lagrange's equations of motion are (Hand, 1998, Page 19)

$$\frac{d}{dt}\left(\frac{\partial\mathcal{L}}{\partial\{\dot{q}_i\}}\right) - \frac{\partial\mathcal{L}}{\partial\{q_i\}} = \{\mathbf{Q}_i\}, \quad i = 1, \dots, n, \tag{14}$$

which can be written as

$$\mathbf{D}(q)\cdot\{\ddot{q}_i\} + \mathbf{C}(q,\dot{q})\cdot\{\dot{q}_i\} + \mathbf{G}(q) = \{\mathbf{Q}_i\}, \tag{15}$$

where $\mathbf{D}(q)$, $\mathbf{C}(q,\dot{q})$, $\mathbf{G}(q)$ and $\{\mathbf{Q}_i\}$ are given in Appendix A.

By multiplying both sides of the equation (15) by the inverse of the inertial matrix $\mathbf{D}^{-1}$, we rewrite equations of dynamics

$$\{\ddot{q}_i\} = \mathbf{D}^{-1}(q)\cdot(\{\mathbf{Q}_i\} - \mathbf{C}(q,\dot{q})\cdot\{\dot{q}_i\} - \mathbf{G}(q))\,. \tag{16}$$

(16) is explicitly written out in Appendix B.

Table 1. Nomenclature for the spherical inverted pendulum

Name	Symbol	Unit	Simulation Value
Generalized Coord.	(x, y, δ, ϵ)	m or rad	-
Shape Variables	$(\delta,\ \epsilon)$	rad	-
External Variables	(x,y)	m	-
The Length	$2\times L$	m	0.6
The Radius	R	m	0.02
The Mass	m	kg	0.35
Gravity	g	m/s^2	9.8
Actuation Forces	$F_x,\ F_y$	N	-
Viscous Fric. Coef.	$C_{x,y}$	$N\cdot s/m$	1×10^{-3}
Viscous Fric. Coef.	C_δ,C_ϵ	$N\cdot s/rad$	1×10^{-3}

We identify an upper triangular structure for the dynamics of the pendulum (16) that is suitable for controller design based on the forwarding tool–nested saturating design. To see that the system is indeed in the upper triangular structure, let $\tilde{\xi}_1 \triangleq (\epsilon, \dot{\epsilon}, \delta, \dot{\delta})$, $\tilde{z}_1 \triangleq \dot{y}$, $\tilde{z}_2 \triangleq \dot{x}$, $\tilde{z}_3 \triangleq y$, and $\tilde{z}_4 \triangleq x$ be the states and $F \triangleq (F_x, F_y)$ be the input. We write the dynamics (16) in a forwarding form :

$$\dot{\tilde{z}}_i = A_i\tilde{z}_i + g_i(\tilde{\xi}_i, F), \quad \dot{\tilde{\xi}}_i = f_i(\tilde{\xi}_i, F), \tag{17}$$

where $i = 1, \dots, 4$, $A_i = 0$, $g_3(\tilde{\xi}_1, F) = \tilde{z}_1$, $g_4(\tilde{\xi}_4, F) = \tilde{z}_2$ and the explicit expression of $g_1(\tilde{\xi}_1, F)$, $g_2(\tilde{\xi}_3, F)$, $f_1(\tilde{\xi}_1, F)$ are obtained from the right hand side of enquations in Appendix B such that $g_1(\tilde{\xi}_1, F) =$ RHS of $\ddot{y}$, $g_2(\tilde{\xi}_3, F) =$ RHS of $\ddot{x}$, $f_1(\tilde{\xi}_1, F) =$ (RHS of $\ddot{\delta}$, RHS of $\ddot{\epsilon}$).

Loosely speaking, system (17) is the upper-triangular structure by considering $\tilde{\xi}_1$ as the first lower subsystem. Strictly speaking, the system must satisfy additional assumptions. For the nested saturating design proposed in Teel (1996), the lower subsystem $\dot{\tilde{\xi}}_i$ must satisfy the asymptotic input to output stable condition. For the Lyapunov based design Mazenc and Praly (1996), the lower subsystem $\dot{\tilde{\xi}}_i$ must the globally asymptotic stable condition. To satisfy these assumptions, one must carry out some preliminary design to the model (17). This task is somewhat complicated because the model has singular points at $\delta = \pi/2 \pm k\pi$ and/or $\epsilon = \pi/2 \pm k\pi$ (referring to Appendix B at the radius $R = 0$) and subsystem $\tilde{\xi}_1$ is not in any particular form. The singularity has physical meaning that when the pendulum is in the horizontal plane, the control signal cannot overcome the gravitational force acting on the pendulum which then will fall. Although we can not apply forwarding immediately, we follow and improve on Liu *et al.* (2005) to recast our problem in such a way that forwarding becomes a feasible approach.

4 Nonlinear Control Design

4.1 *Overview of the Design Procedure*

The forwarding controller for the planar pendulum proposed in Angeli (2001b); Teel (1996) can be extended to the spherical inverted pendulum as has been suggested in Angeli (2001a). Here we formulate a full forwarding controller for the spherical inverted pendulum as is illustrated in the conference version of this paper Liu *et al.* (2005).

Define $U \triangleq \{(x, \dot{x}, y, \dot{y}, \delta, \dot{\delta}, \epsilon, \dot{\epsilon}) \in R^8 | -\frac{\pi}{2} < \delta < \frac{\pi}{2}, -\frac{\pi}{2} < \epsilon < \frac{\pi}{2}\}$ to denote the upper hemisphere of the pendulum. For simplicity of the design, we let the radius of the pendulum $R = 0$ and the exogenous input $v_f = 0$, that is, in the design, we consider the generalized control force[1]

$$\{Q\} = \big(F_x,\ F_y,\ 0,\ 0\big)\,. \tag{18}$$

The control design proceeds by first simplifying the dynamics using partial state feedback linearization. Next, we map the upper hemisphere U into R^8, to eliminate the problem in the $x - y$ plane. The system is ready for the forwarding design. Moreover, this has the added advantage of minimizing the number of forwarding steps that need to be carried out, which assists the transient performance of the controller.

4.2 *Design Step 1*

We recall that the nominal dynamics (16) with $R = 0$ and $v_f = 0$ can be written in the form (1) as follows

$$\begin{aligned}
\begin{pmatrix} \ddot{x} \\ \ddot{y} \\ \hline \ddot{\delta} \\ \ddot{\epsilon} \end{pmatrix} &= \begin{pmatrix} g_{x1}(\delta,\epsilon) & g_{x2}(\delta,\epsilon) \\ g_{y1}(\delta,\epsilon) & g_{y2}(\delta,\epsilon) \\ \hline g_{\delta 1}(\delta,\epsilon) & g_{\delta 2}(\delta,\epsilon) \\ g_{\epsilon 1}(\delta,\epsilon) & g_{\epsilon 2}(\delta,\epsilon) \end{pmatrix} \begin{pmatrix} F_x \\ F_y \end{pmatrix} + \begin{pmatrix} f_x(\delta,\dot{\delta},\epsilon,\dot{\epsilon}) \\ f_y(\delta,\dot{\delta},\epsilon,\dot{\epsilon}) \\ \hline f_\delta(\delta,\dot{\delta},\epsilon,\dot{\epsilon}) \\ f_\epsilon(\delta,\dot{\delta},\epsilon,\dot{\epsilon}) \end{pmatrix} \\
&\triangleq \begin{pmatrix} H_{11}(\delta,\epsilon) \\ \hline H_{21}(\delta,\epsilon) \end{pmatrix} F + \begin{pmatrix} H_{12}(\delta,\dot{\delta},\epsilon,\dot{\epsilon}) \\ \hline H_{22}(\delta,\dot{\delta},\epsilon,\dot{\epsilon}) \end{pmatrix}\,,
\end{aligned} \tag{19}$$

where $H_{21}(\delta, \epsilon)$ are invertible on U and $H_{11}(\delta, \epsilon)$, $H_{21}(\delta, \epsilon)$, $H_{12}(\delta, \dot{\delta}, \epsilon, \dot{\epsilon})$, $H_{22}(\delta, \dot{\delta}, \epsilon, \dot{\epsilon})$ are explicitly given in Appendix C.

The following result converts the nominal system (19) to a globally defined upper triangular structure.

LEMMA 4.1 *Consider the dynamics (19). There exists a map $T : U \to R^8$ such that using the state transformation*

$$(z, \xi_1) = T(q, \dot{q})\,, \tag{20}$$

[1] But, R and v_f are not zero for the nonlinear dynamics of the pendulum in the simulations such that the robustness of the proposed controller will be tested.

where $z \in R^4$, $\xi_1 \in R^4$ and a feedback transformation

$$F = H_{21}^{-1}(\delta,\epsilon) \cdot \left(H_{31}^{-1}(\delta,\epsilon) \cdot (u - H_{32}(\delta,\dot{\delta},\epsilon,\dot{\epsilon})) - H_{22}(\delta,\dot{\delta},\epsilon,\dot{\epsilon}) \right), \tag{21}$$

where u is the new control and

$$H_{31}(\delta,\epsilon) \triangleq \begin{pmatrix} 1+\tan^2(\delta) & 0 \\ 0 & 1+\tan^2(\epsilon) \end{pmatrix},$$

$$H_{32}(\delta,\dot{\delta},\epsilon,\dot{\epsilon}) \triangleq \begin{pmatrix} 2\dot{\delta}^2 \tan(\delta)(1+\tan^2(\delta)) \\ 2\dot{\epsilon}^2 \tan(\epsilon)(1+\tan^2(\epsilon)) \end{pmatrix},$$

system (16) is transformed to an appropriate upper triangular form in R^8,

$$\begin{aligned} \dot{z}_i &= A_i z_i + g_i(\xi_i, u) \\ \dot{\xi}_i &= f_i(\xi_i, u) \qquad \text{for } i = 1,2,3,4 \end{aligned} \tag{22}$$

where $A_i = 0$, $z \triangleq (z_1, z_2, z_3, z_4)$, $\xi_1 \triangleq (\xi_{11}, \xi_{12}, \xi_{13}, \xi_{14})$, $\xi_{j+1} \triangleq (\xi_j, z_j)$ for $j = 1,2,3,4$, $g_4(\xi_4, u) \triangleq z_2$, $g_3(\xi_3, u) \triangleq z_1$,

$$\begin{aligned} \begin{pmatrix} g_2(\xi_1,u) \\ g_1(\xi_1,u) \end{pmatrix} \triangleq\ & H_{11}(T^{-1}(z,\xi_1)) \cdot \left(H_{21}^{-1}(T^{-1}(z,\xi_1)) \cdot \left(H_{31}^{-1}(T^{-1}(z,\xi_1)) \cdot (u - H_{32}(T^{-1}(z,\xi_1))) \right.\right. \\ & \left.\left. - H_{22}(T^{-1}(z,\xi_1)) \right)\right) + H_{12}(T^{-1}(z,\xi_1)), \end{aligned}$$

with the mapping $H_{ij}(q,\dot{q}) \rightarrow H_{ij}(T^{-1}(z,\xi_1))$, and subsystem $\dot{\xi}_1 = f_1(\xi_i, u)$ is defined as follows $(\dot{\xi}_{14}, \dot{\xi}_{13}, \dot{\xi}_{12}, \dot{\xi}_{11}) = (\xi_{13}, u_1, \xi_{11}, u_2)$.

Proof First, we use partial feedback linearization to better see how the angle acceleration $(\ddot{\delta}, \ddot{\epsilon})$ can be controlled.

We consider a partial input-output feedback linearization. Let the output vector be (x, y, δ, ϵ). We have

$$\begin{pmatrix} \ddot{x} \\ \ddot{y} \\ \ddot{\delta} \\ \ddot{\epsilon} \end{pmatrix} = \begin{pmatrix} H_{11}(\delta,\epsilon) \\ H_{21}(\delta,\epsilon) \end{pmatrix} F + \begin{pmatrix} H_{12}(\delta,\dot{\delta},\epsilon,\dot{\epsilon}) \\ H_{22}(\delta,\dot{\delta},\epsilon,\dot{\epsilon}) \end{pmatrix}, \tag{23}$$

which implies that system (19) has a vector relative degree $(2,2,2,2)$. $\begin{pmatrix} H_{11}(\delta,\epsilon) \\ H_{21}(\delta,\epsilon) \end{pmatrix}$ is not square because of the underactuated system (19), i.e., $F \in R^2$, $q \in R^4$. We may achieve partial feedback linearization, for example,

$$F = H_{21}^{-1}(\delta,\epsilon)(\nu - H_{22}(\delta,\epsilon)), \tag{24}$$

where $\nu = (\nu_1, \nu_2)$ is a new input vector. This leads us to

$$\begin{pmatrix} \ddot{x} \\ \ddot{y} \\ \ddot{\delta} \\ \ddot{\epsilon} \end{pmatrix} = \begin{pmatrix} H_{11}(\delta,\epsilon) \cdot H_{21}^{-1}(\delta,\epsilon)(\nu - H_{22}(\delta,\dot{\delta},\epsilon,\dot{\epsilon})) + H_{12}(\delta,\dot{\delta},\epsilon,\dot{\epsilon}) \\ \hline \nu \end{pmatrix}. \tag{25}$$

Next, introduce variables:

$$(z_4,\, z_3,\, z_2,\, z_1,\, \xi_{14},\, \xi_{13},\, \xi_{12},\, \xi_{11}) = (x,\, y,\, \dot{x},\, \dot{y},\, \tan(\delta),\, (1+\tan^2(\delta))\dot{\delta},\, \tan(\epsilon),\, (1+\tan^2(\epsilon))\dot{\epsilon})\,,$$

and a change of control input

$$\begin{aligned} u &= \begin{pmatrix} 1+\tan^2(\delta) & 0 \\ 0 & 1+\tan^2(\epsilon) \end{pmatrix} \nu + \begin{pmatrix} 2\dot{\delta}^2 \tan(\delta)(1+\tan^2(\delta)) \\ 2\dot{\epsilon}^2 \tan(\epsilon)(1+\tan^2(\epsilon)) \end{pmatrix} \\ &\triangleq H_{31}(\delta,\epsilon)\nu + H_{32}(\delta,\dot{\delta},\epsilon,\dot{\epsilon})\,. \end{aligned} \tag{26}$$

Clearly, $H_{31}(\delta,\epsilon)$ is invertible for $(\delta,\epsilon) \in \left(-\frac{\pi}{2},\frac{\pi}{2}\right)$ and $u = (u_1, u_2)$ is a new input vector. □

Remark 1 Notice that system (25) does not modify the upper triangular structure (17). Actually, the forwarding design in Liu *et al.* (2005) is carried out by taking advantage of the upper triangular structure (25), where the stability for linear subsystem $\tilde{\xi}_1 = (\delta, \dot{\delta}, \epsilon, \dot{\epsilon})$ is established by LaSalle's invariance principle which is regarded as an extension of the design for planar inverted pendulum in Teel (1996). Instead, we formulate the controller here based on system (22), which is defined globally, such that some improvements are expected. In particular, it enables us to use an ISS-Lyapunov function to obtain asymptotic gains.

Remark 2 Obviously, one can proceed directly using the standard forwarding design tools by either Lyapunov based design or nested saturating design to the upper triangular form (22). However the blind application of the standard Lyapunov forwarding designs runs into difficulty. Indeed, the requirement to solve recursively some rather general and highly nonlinear PDE is less than attractive.

Remark 3 The straightforward application of nested saturating design leads to excessively poor transient behaviour. To alleviate this, we use a high gain design to regulate the angle related variables and use the forwarding design only for the remaining variables. This provides a reasonable compromise between speed of convergence and robustness as will be illustrated in Section 5.

4.3 *Design Step 2*

We develop a controller for the subsystem with the states ξ_1 (the modified shape variables). The dynamics are governed by two independent pairs of double integrators. We may assign a linear control law as follows

$$\begin{aligned} u &= \begin{pmatrix} -\kappa^2 k_4 \xi_{14} - \kappa k_3 \xi_{13} \\ -\kappa^2 k_2 \xi_{12} - \kappa k_1 \xi_{11} \end{pmatrix} + \begin{pmatrix} v_1^x \\ v_1^y \end{pmatrix} \\ &\triangleq f_u + v_1\,, \end{aligned} \tag{27}$$

where $v_1 = (v_1^x, v_1^y)$ is a new input vector and $k_i > 0$, for $i = 1,2,3,4$, $\kappa > 0$ are design parameters.

In what follows, we show that the closed loop system ξ_1 with the control function (27) satisfies asymptotic (input v_1 to output $y = \xi_1$) gains by choosing appropriate parameters. The result enables us to apply the forwarding tool for the rest.

To this end, and without loss of generality, we study the linear system

$$\dot{x} = Ax + \Delta\,, \tag{28}$$

where $A = \begin{pmatrix} 0 & 1 \\ -\kappa^2 L_1 & -\kappa L_2 \end{pmatrix}$ and input $\Delta \in R^2$. The eigenvalues of A are $\lambda_{1,2} = -\kappa a_{1,2}$ where $a_1 = \frac{L_2+\sqrt{L_2^2-4L_1}}{2}$ and $a_2 = \frac{L_2-\sqrt{L_2^2-4L_1}}{2}$. If we let $L_2^2 > 4L_1$, we have $a_1 > a_2 > 0$. The next result shows that system (28) is asymptotic input to output stable with input Δ. Moreover, the parameter κ can be used to tune the asymptotic gains.

Lemma 4.2 *Consider system (28). Assume that the following conditions* $L_2^2 - 4L_1 > 0$, $\|\Delta_1\|_a \le \Delta_{1,M}$ *and* $\|\Delta_2\|_a \le \Delta_{2,M}$ *hold for positive numbers* L_1, L_2, $\Delta_{1,M}$ *and* $\Delta_{2,M}$. *Then, for some class* $\mathcal{K}$ *functions* γ_{11}, γ_{12}, γ_{21} *and* γ_{22}, *system (28) satisfies an asymptotic input to output bound, without restriction on initial states, with restriction on exogenous inputs* Δ_1 *and* Δ_2, *and with linear asymptotic gains*

$$\begin{aligned}\|x_1\|_a &\le \max\{\gamma_{11}(\|\Delta_1\|_a),\ \gamma_{12}(\|\Delta_2\|_a)\}\\ \|x_2\|_a &\le \max\{\gamma_{21}(\|\Delta_1\|_a),\ \gamma_{22}(\|\Delta_2\|_a)\}\end{aligned} \tag{29}$$

where for some $\varrho \in (0,1)$,

$$\begin{cases}\gamma_{11}(r) = \frac{1}{1-\varrho}\left|\frac{4(L_2+\sqrt{L_2^2-4L_1})}{\kappa(L_2-\sqrt{L_2^2-4L_1})\sqrt{L_2^2-4L_1}}\right| r\\ \gamma_{12}(r) = \frac{1}{1-\varrho}\left|\frac{8}{\kappa^2(L_2-\sqrt{L_2^2-4L_1})\sqrt{L_2^2-4L_1}}\right| r\\ \gamma_{21}(r) = \frac{1}{1-\varrho}\left|\frac{2(L_2+\sqrt{L_2^2-4L_1})}{\sqrt{L_2^2-4L_1}}\right| r\\ \gamma_{22}(r) = \frac{1}{1-\varrho}\left|\frac{4}{\kappa\sqrt{L_2^2-4L_1}}\right| r\end{cases} \tag{30}$$

Proof Consider $x = Py$ with $P = \begin{pmatrix} 1 & 1 \\ -\kappa a_1 & -\kappa a_2\end{pmatrix}$. System (28) transforms to

$$\dot{y} = P^{-1}(APy + \Delta) \stackrel{\triangle}{=} By + \bar{\Delta} \tag{31}$$

where $B = \begin{pmatrix} -\kappa a_1 & 0 \\ 0 & -\kappa a_2\end{pmatrix}$ and $\bar{\Delta} = \begin{pmatrix} \frac{-a_2}{a_1-a_2}\Delta_1 + \frac{-1}{\kappa(a_1-a_2)}\Delta_2 \\ \frac{a_1}{a_1-a_2}\Delta_1 + \frac{1}{\kappa(a_1-a_2)}\Delta_2\end{pmatrix}$. System (31) is considered as two decoupled subsystems with the external inputs $\bar{\Delta}$.

Let the Lyapunov candidate $V_1 = \frac{1}{2}y_1^2$ and $V_2 = \frac{1}{2}y_2^2$ for subsystems $\dot{y}_1$ and $\dot{y}_2$ respectively. Next, we make V_1 and V_2 ISS-Lyapunov functions to obtain the ISS gains for system (31). Then, we summarize the asymptotic gains for system (31) from the ISS gains. Choose class $\mathcal{K}_\infty$ functions $\overline{\alpha}(r) = \frac{1}{2}r^2$ and $\underline{\alpha} = \frac{1}{2}r^2$ such that $\overline{\alpha}(|y_1|) = V_1 = \underline{\alpha}(|y_1|)$, $\overline{\alpha}(|y_2|) = V_2 = \underline{\alpha}(|y_2|)$.

The time derivative of V_1 along the trajectory of system (31) is given by

$$\begin{aligned}\frac{\partial V_1}{\partial y_1}(By + \bar{\Delta}) &\le -\left(\kappa a_1 - \frac{\bar{\Delta}_1}{|y_1|}\right) y_1^2 \quad (y_1 \ne 0)\\ &\stackrel{\triangle}{=} -\alpha_0 y_1^2.\end{aligned} \tag{32}$$

To make the right hand side of the inequality (32) negative definite, we require $\alpha_0 > 0$, which is guaranteed by

$$|y_1| \ge \frac{1}{(1-\varrho)\kappa a_1}\left|\bar{\Delta}_1\right| \tag{33}$$

for some $\varrho \in (0,1)$, where $\bar{\Delta}_1 = -\frac{a_2\Delta_1}{a_1-a_2} - \frac{\Delta_2}{\kappa(a_1-a_2)}$. Let $\alpha_1(r) \stackrel{\triangle}{=} \alpha_0 r^2$ be a class $\mathcal{K}_\infty$ function. Because $\overline{\alpha}(r)$ and $\underline{\alpha}(r)$ are also class $\mathcal{K}_\infty$ functions, by definition, V_1 is an ISS-Lyapunov function. According to Theorem 2.1, the subsystem y_1 is ISS. Then, there exists a class $\mathcal{KL}$ function $\beta(r,t)$ and a class $\mathcal{K}$ function $\bar{\gamma}(r) \stackrel{\triangle}{=} \underline{\alpha}^{-1} \circ \overline{\alpha} \circ \frac{1}{(1-\varrho)\kappa a_1} r = \frac{1}{(1-\varrho)\kappa a_1} r$ such that $\|y_1(t)\| \le \max\{\beta(\|x(0)\|, t), \bar{\gamma}(\|\bar{\Delta}_1\|_\infty)\}$ (see (Isidori, 1999, page 21)). As $t \to \infty$, the class $\mathcal{KL}$ function $\beta(\|x(0)\|, t) \to 0$ and we obtain an asymptotic gain $\|y_1(t)\|_a \leq \bar{\gamma}(\|\bar{\Delta}_1\|_a)$. Then, we conclude an asymptotic gain for y_1 as follows

$$\|y_1\|_a \leq \max\{\bar{\gamma}_{11}(\|\Delta_1\|_a),\ \bar{\gamma}_{12}(\|\Delta_2\|_a)\} \tag{34}$$

where $\bar{\gamma}_{11}(r) \triangleq \frac{1}{1-\varrho}\left|\frac{2a_2}{\kappa a_1(a_1-a_2)}\right| r$, $\bar{\gamma}_{12}(r) \triangleq \frac{1}{1-\varrho}\left|\frac{2}{\kappa^2 a_1(a_1-a_2)}\right| r$.

Similarly, we take the time derivative of V_2 along the trajectory of system (31) and obtain an asymptotic gain for y_2 as follows

$$\|y_2\|_a \leq \max\{\bar{\gamma}_{21}(\|\Delta_1\|_a),\ \bar{\gamma}_{22}(\|\Delta_2\|_a)\} \tag{35}$$

where we define $\bar{\gamma}_{21}(r) \triangleq \frac{1}{1-\varrho}\left|\frac{2a_1}{\kappa a_2(a_1-a_2)}\right| r$, $\bar{\gamma}_{22}(r) \triangleq \frac{1}{1-\varrho}\left|\frac{2}{\kappa^2 a_2(a_1-a_2)}\right| r$.

Next, we cast the asymptotic gains for y into the asymptotic gains for x. It is easy to check that the inequality $\|x_1\|_a = \|y_1\|_a + \|y_2\|_a \leq \max\{\gamma^*_{11}(\|\Delta_1\|_a), \gamma^*_{12}(\|\Delta_2\|_a)\}$ with $\gamma^*_{11}(r) \triangleq 2\bar{\gamma}_{21}(r)$ and $\gamma^*_{21}(r) \triangleq 2\bar{\gamma}_{22}(r)$ is satisfied because by condition $a_1 > a_2 > 0$, $\bar{\gamma}_{21}(r) > \bar{\gamma}_{11}(r)$ and $\bar{\gamma}_{22}(r) > \bar{\gamma}_{12}(r)$ hold. Furthermore, we have $\|x_2\|_a = \kappa a_1\|y_1\|_a + \kappa a_2\|y_2\|_a \leq \max\{\gamma^*_{21}(\|\Delta_1\|_a), \gamma^*_{22}(\|\Delta_2\|_a)\}$ where we define $\gamma^*_{21}(r) \triangleq \frac{1}{1-\varrho}\left|\frac{4a_1}{a_1-a_2}\right| r$, $\gamma^*_{22}(r) \triangleq \frac{1}{1-\varrho}\left|\frac{4}{\kappa(a_1-a_2)}\right| r$. Substituting the functions of a_1 and a_2 to class $\mathcal{K}$ functions $\gamma^*_{11}(r)$, $\gamma^*_{12}(r)$, $\gamma^*_{21}(r)$ and $\gamma^*_{22}(r)$ gives the asymptotic gains for $\|x_1\|_a$ and $\|x_2\|_a$. □

Remark 4 Lemma (4.2) not only parameterizes the asymptotic gains from inputs to states but also shows that κ can be used as a key parameter to tune the gains γ_{11}, γ_{12}, γ_{22}. In our case, we have $\Delta_1 = 0$ and hence $\gamma_{21}(\|\Delta_1\|_a) = 0$ because the exogenous inputs only appear at the dynamics $\ddot{\delta}$ (or $\ddot{\epsilon}$). Furthermore, we let $\Delta_2 = v_1^y$ (or $\Delta_2 = v_1^x$) in subsystem ξ_1 for the purpose of recursive forwarding design. Therefore, we only need gains γ_{12}, γ_{22} which are tunable by κ.

4.4 *Design Steps 3-6*

By applying Theorem 2.2 repeatedly, we can obtain a nested saturating controller for each augmented system ξ_{i+1}, $i = 1, \ldots, 4$ of (22).

The design task is to design a saturation function for v_i, $i = 1, \ldots, 4$ such that $\alpha_i(\xi_i, v_i)$, $i = 1, \ldots, 4$ with the external input $v_i \triangleq (v_i^x,\ v_i^y)$, $i = 1, \ldots, 4$ ensures that the augmented system

$$f_{i+1}(\xi_{i+1}, \alpha_i(\cdot,\cdot)) = \begin{pmatrix} A_i z_i + g_i(\xi_i, \alpha_i(\cdot,\cdot)) \\ f_i(\xi_i, \alpha_i(\cdot,\cdot)) \end{pmatrix}, \tag{36}$$

satisfies an asymptotic input-output bound.

In each step of the recursive design, we must make sure that all conditions in Theorem 2.2 hold. Assumption (i) holds as $A_i = 0$, $i = 1, \ldots, 4$. Notice that the linear approximation of each augmented system at the equilibrium $(z_i, \xi_i, v_i) = (0, 0, 0)$, $i = 1, \ldots, 4$ is stabilizable. Thus, Assumption (ii) holds. Assumptions (iiia-c) are automatically satisfied because they are the results of the previous design step. In summary, all conditions are satisfied.

Now, we can apply the Theorem 2.2 to design a complete control law for the pendulum. Noting that (F_{i+1}, G_{i+1}), $i = 1, \ldots, 4$ is stabilizable, we employ a LQR design for all recursive design steps and obtain the optimal gain matrices K_{i+1}, $i = 1, \ldots, 4$ such that the controller $v_i = K_{i+1}\xi_{i+1}$ minimizes the cost function

$$J(\xi_{i+1}, v_i) = \int_0^\infty (\xi_{i+1}^T Q \xi_{i+1} + v_i^T R v_i) dt, \tag{37}$$

where Q and R are weight matrices. All eigenvalues of $(F_{i+1} + G_{i+1}K_{i+1})$ are in C^-.

Let $\Omega_i = 0$, $i = 2, \ldots, 5$. Finally, a nested saturating controller for the transformed upper triangular system (22) is obtained

$$u \overset{\triangle}{=} f_u + \sigma_{i+1}\,, \tag{38}$$

for $i = 1, \ldots, 4$, where $\sigma_{i+1} \overset{\triangle}{=} \lambda_{i+1}\sigma\left(\frac{1}{\lambda_{i+1}}\left(K_{i+1}\xi_{i+1} + \Gamma_{i+1}v_{i+1}\right)\right)$, $v_{i+1} = \sigma_{i+2}$. To make the controller simple, we set $\Gamma_i = \mathbf{I}$, $i = 2, \ldots, 5$. λ_i, $i = 2, \ldots, 5$, are adjustable parameters in the proposed controller. With $\kappa = 1$, $k_2 = k_4 = 100(N/rad)$, $k_1 = k_3 = 20(N/rad \cdot s)$, we may obtain K_i, for $i = 2, 3, 4, 5$. Explicit expression are given in Appendix D.

The control law for the original dynamics (16) is given by substituting the function (38) with the mapping to the original coordinates $(q, \dot{q})$ into the control function (21),

$$\begin{aligned} F = H_{21}^{-1}(\delta,\epsilon)\cdot\Bigg(&-H_{22}(\delta,\dot\delta,\epsilon,\dot\epsilon) + H_{31}^{-1}(\delta,\epsilon)\cdot\Bigg(-H_{32}(\delta,\dot\delta,\epsilon,\dot\epsilon) + \begin{pmatrix} -\kappa^2k_4\tan(\delta) - \kappa k_3(1+\tan^2(\delta))\dot\delta \\ -\kappa^2k_2\tan(\epsilon) - \kappa k_1(1+\tan^2(\epsilon))\dot\epsilon \end{pmatrix} \\ &+\lambda_2\sigma\left(\frac{1}{\lambda_2}\left(K_2\xi_2 + \lambda_3\sigma\left(\frac{1}{\lambda_3}\left(K_3\xi_3 + \lambda_4\sigma\left(\frac{1}{\lambda_4}\left(K_4\xi_4 + \lambda_5\sigma\left(\frac{1}{\lambda_5}\left(K_5\xi_5\right)\right)\right)\right)\right)\right)\right)\right)\Bigg)\Bigg)\,, \end{aligned} \tag{39}$$

where H_{ij} for $i = 2, 3$, $j = 1, 2$ are functions of $(\delta, \dot\delta, \epsilon, \dot\epsilon)$ (referring to Appendix C and the proof in Lemma 4.1), $\xi_2 \overset{\triangle}{=} (\dot y,\ \tan(\delta),\ (1+\tan^2(\delta))\dot\delta,\ \tan(\epsilon),\ (1+\tan^2(\epsilon))\dot\epsilon)$, $\xi_3 \overset{\triangle}{=} (\dot x,\ \dot y,\ \tan(\delta),\ (1+\tan^2(\delta))\dot\delta,\ \tan(\epsilon),\ (1+\tan^2(\epsilon))\dot\epsilon)$, $\xi_4 \overset{\triangle}{=} (y,\ \dot x,\ \dot y,\ \tan(\delta),\ (1+\tan^2(\delta))\dot\delta,\ \tan(\epsilon),\ (1+\tan^2(\epsilon))\dot\epsilon)$, $\xi_5 \overset{\triangle}{=} (x,\ y,\ \dot x,\ \dot y,\ \tan(\delta),\ (1+\tan^2(\delta))\dot\delta,\ \tan(\epsilon),\ (1+\tan^2(\epsilon))\dot\epsilon)$.

The designed controller yields:

THEOREM 4.3 *Consider the dynamics (19) for the spherical inverted pendulum. Assume that all conditions in Lemma 4.1 and Lemma 4.2 are satisfied. The control function F is defined in (39). Then, the trajectories of the closed loop system (19) converge to the origin as $t \to \infty$ for all trajectories starting in the set U.*

Proof The result follows from the construction of the control law (39). □

Remark 5 Notice structure of the control law (39), it consists of two different actions: (i) a high gain action to compensate the angular deviations (the non-saturated part in (39)); (ii) a low gain action to compensate the position errors (the saturated part in (39)).

Remark 6 One could have designed the entire controller using the forwarding principle. This would have lead to a very conservative design with an unnatural time-scale separation between angular variables. in our design, this has been avoided by designing first a high gain feedback loop to regulate the angular variables (*Design Step 2*). This first control step has the added advantage of yielding an ISS property from disturbances to angular variables (see proof of Lemma 4.2). This is more than what is required in Theorem 2.2 to enable nested saturation design to proceed with *Design Step 3-6*. Indeed, Theorem 2.2 only require asymptotic gain (29), which is trivially satisfied by ISS. The control design (*Step 2-6*) yields, according to Theorem 2.2, a closed loop where the upright equilibrium is stable and the closed loop has asymptotic gain from any sufficiently small disturbances to the state.

Remark 7 The proposed controller yields a robust closed loop system in that the controlled system satisfies an asymptotic input-to-state bound for sufficiently small exogenous disturbances, ($v_5(\cdot)$ limited by $\delta' > 0$). By tuning the asymptotic gains (see Lemma 4.2) it may be possible to achieve a large δ'. The precise characterization of the robustness properties is however difficult. In order to gain insight into the robustness properties of the controlled system we use a simulation study in the next section.

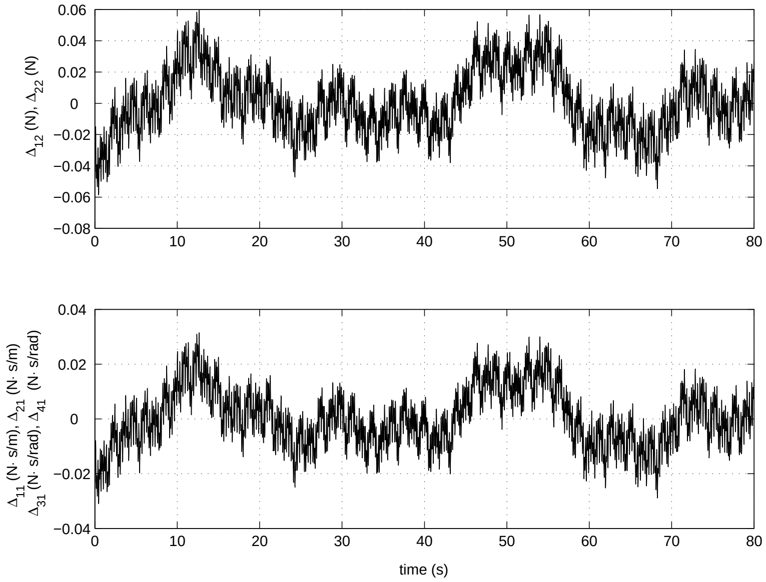

Figure 2. Exogenous disturbances

5 Advanced Simulation Studies

The controlled system behaviour is evaluated through computer simulation. The nonlinear model, used as the plant, takes into account the full three dimensional structure of the slim beam ($R = 0.02$ (m) and $2L = 0.6$ (m)) as well as some exogenous forces (e.g., viscous friction, input noises) both of which have been neglected in the design.

Let $\lambda_2 = 5$, $\lambda_3 = 4.5$, $\lambda_4 = 3$, $\lambda_5 = 2.5$, $v_5(\cdot) = 0$, for our design.

Let the exogenous inputs be as follows,

$$v_f = \big((-C_x + \Delta_{11})\dot{x} + \Delta_{12}\,,\, (-C_y + \Delta_{21})\dot{y} + \Delta_{22}\,,\, (-C_\delta + \Delta_{31})\dot{\delta}\,,\, (-C_\epsilon + \Delta_{41})\dot{\delta} \big) \tag{40}$$

where $\Delta_{ij} \triangleq \sum_{k=1}^{M} a_{k,ij} \sin(\omega_{k,ij} t + \varphi_{k,ij})$ for $i = 1, 2, 3, 4$ and $j = 1, 2$ with real number $a_{k,ij}$, $\omega_{k,ij}$, $\varphi_{k,ij}$, $k = 1, \ldots, M$ are the external disturbances. The root mean square value–RMS of the exogenous disturbances Δ_{ij} for $i = 1, 2, 3, 4$ and $j = 1, 2$ is given by

$$\begin{aligned} \mathrm{RMS}_{\Delta_{ij}} &\triangleq \sqrt{\lim_{T\to\infty} \frac{1}{T} \int_0^T \Delta_{ij}^2(t)dt} \\ &= \sqrt{\frac{1}{2} \sum_{k=1}^{M} a_{k,ij}^2} \end{aligned} \tag{41}$$

The exogenous disturbances (40) together with the proposed control function (39) serve as the generalized input $\{Q\}$ to the plant

$$\{Q\} = \big(F_x,\ F_y,\ 0,\ 0 \big) + v_f\,. \tag{42}$$

In the sequel we omit to mention the units for brevity sake. We use for $(x, \dot{x}, y, \dot{y}, \delta, \dot{\delta}, \epsilon, \dot{\epsilon})$ the units (m, m/s, m, m/s, rad, rad/s, rad, rad/s) respectively. All forces are measured in N (Newtons). Time is measured in s (second). In Figures 6, 7, 8, 9, we use degrees instead of radians to measure the angles.

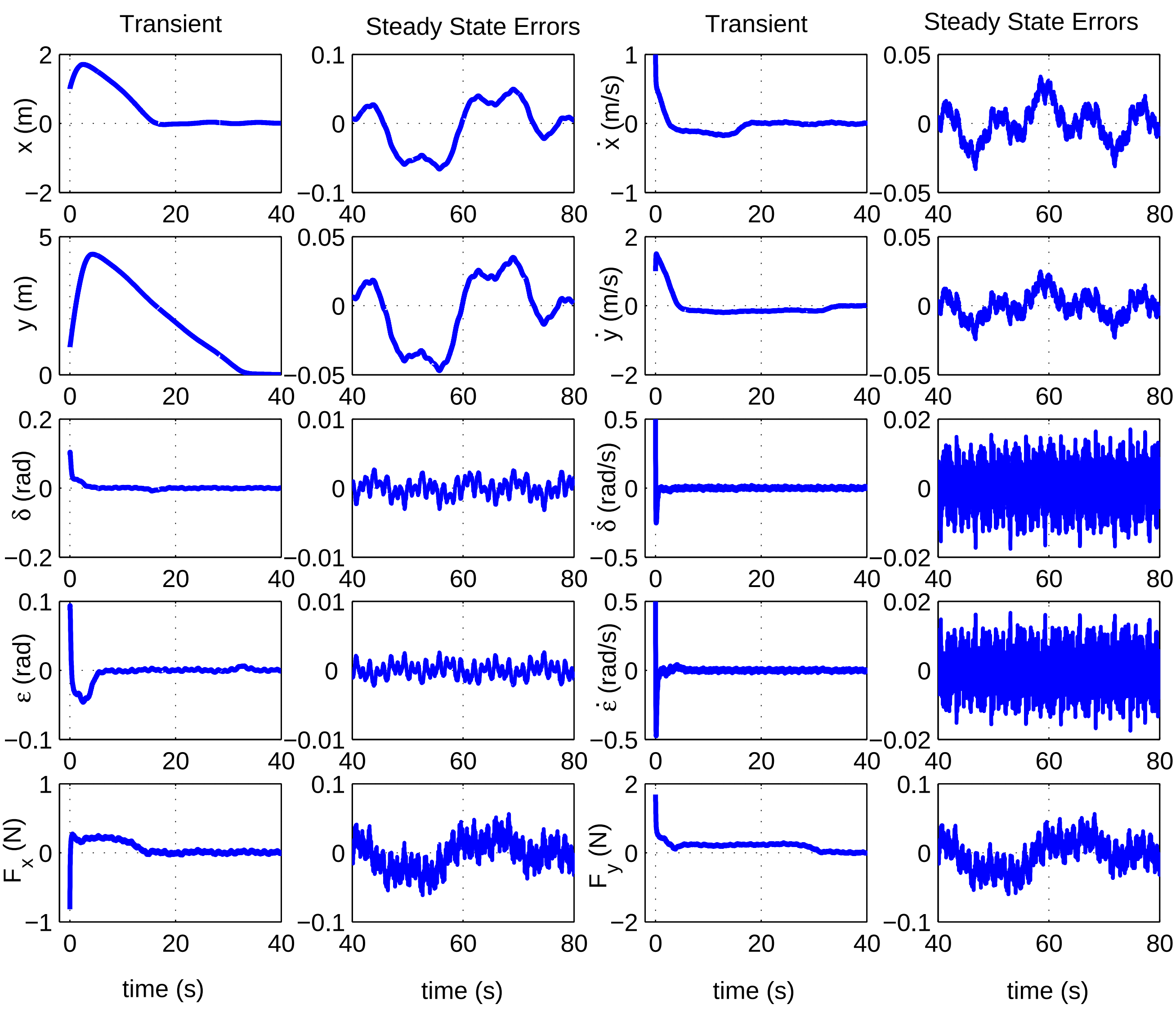

Figure 3. Simulation Results for *Case 1*

5.1 *Some Individual Responses*

Let RMS for Δ_{i1} with $i = 1, 2$ be $0.01\,(N \cdot s/m)$. Let RMS for Δ_{i1} with $i = 3, 4$ be $0.01\,(N \cdot s/rad)$. Let RMS for Δ_{i2} with $i = 1, 2$ be $0.02\,(N)$. Figure 2 shows the signals Δ_{ij} for $i = 1, 2, 3, 4$ and $j = 1, 2$, the exogenous disturbances, which are used in simulations.

Case 1: The initial state is: $(x(0), \dot{x}(0), y(0), \dot{y}(0), \delta(0), \dot{\delta}(0)\epsilon(0), \dot{\epsilon}(0)) = (1\,, 1\,, 1\,, 1\,, 0.087\,, 0.5\,, 0.087\,, 0.5)$. The simulation results are shown in Figure 3, which show the transient as well as steady state response for each state variable. Observe the fast regulation of the angular variables compared to the much slower response of the position $(x, \dot{x}, y, \dot{y})$ variables.

Case 2: Let the initial state be: $(x(0), \dot{x}(0), y(0), \dot{y}(0), \delta(0), \dot{\delta}(0)\epsilon(0), \dot{\epsilon}(0)) = (20\,, 5\,, 20\,, 5\,, 0.384\,, 0.5\,, 0.524\,, 0.5)$, where small angular deviation with large initial angular velocity is given. The simulation results are shown in Figure 4.

Case 3: The initial state is given by $(x(0), \dot{x}(0), y(0), \dot{y}(0), \delta(0), \dot{\delta}(0)\epsilon(0), \dot{\epsilon}(0)) = (1000\,, 10\,, 1000\,, 10\,, 0.524\,, 5\,, 1.222\,, 5)$. The simulation results are presented in Figure 5. Notice how slow the states (x, y) converge towards the origin in Figure 5.

The angular variables are tightly regulated, where the design uses high gain feedback. The translational variables are more slowly regulated. The control law uses low gain feedback for these variables.

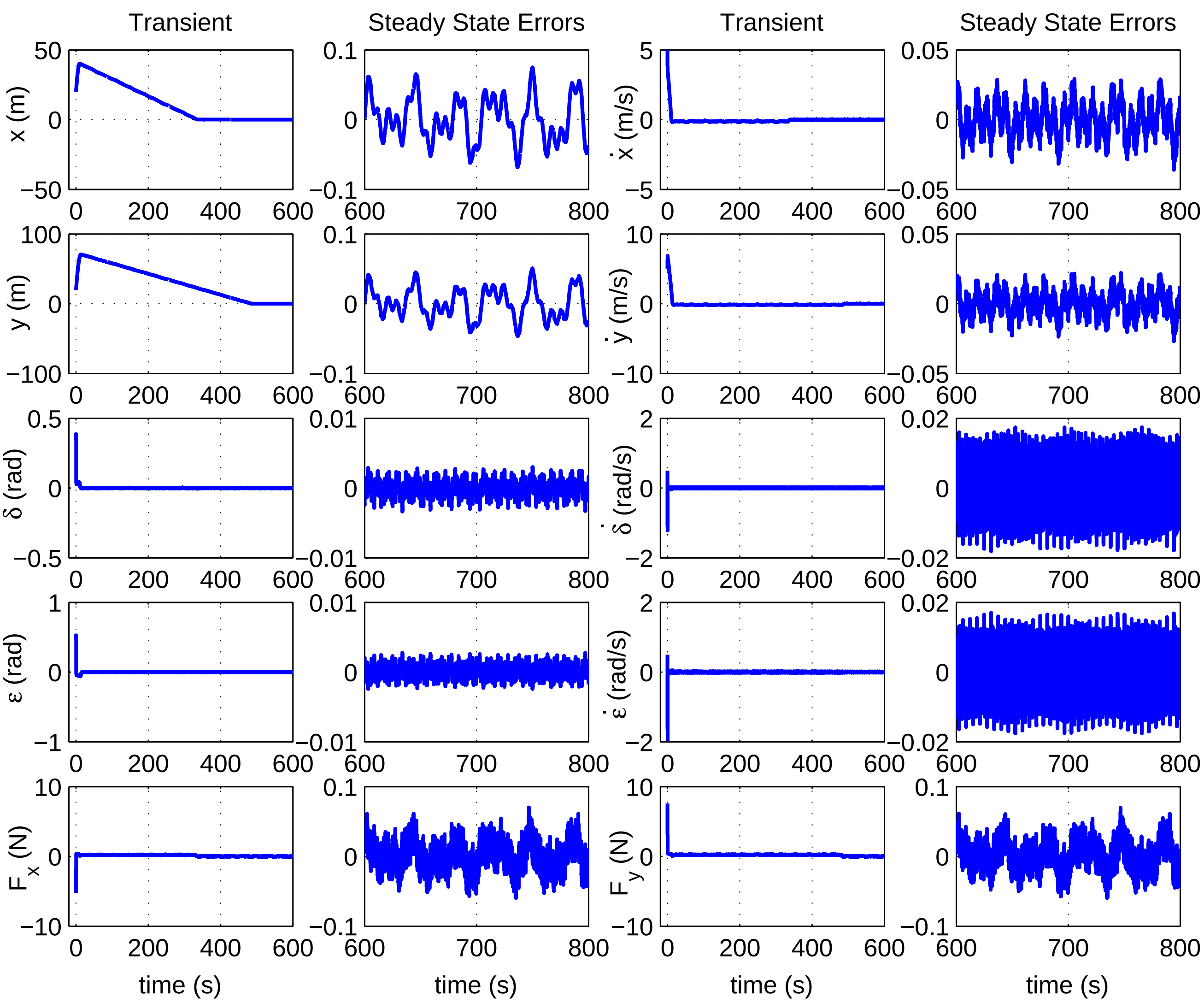

Figure 4. Simulation Results for *Case 2*

5.2 *Control Force Response*

Clearly, angular deviations are key as far as the total control force that is required to maintain posture control. To illustrate this point, a series of simulations are performed with initial conditions $(x(0), \dot{x}(0), y(0), \dot{y}(0), \delta(0), \dot{\delta}(0), \epsilon(0), \dot{\epsilon}(0)) = (0\,,0\,,0\,,0\,,\delta(0)\,,0\,,\epsilon(0)\,,0)$, where $\delta(0) \in \{0°, 3°, \ldots, 45°\}$ and $\epsilon(0) \in \{0°, 3°, \ldots, 45°\}$.

From these simulations, we extract a relationship between (δ, ϵ) and $\|F\|_\infty \triangleq \sup_{t>0} \|F(t)\|$ with $\|F(t)\| = \sqrt{(F_x(t))^2 + (F_y(t))^2}$.

Figure 6 shows that $\|F\|_\infty$ against the initial deviation angles (δ, ϵ). As is to be expected, $\|F\|_\infty$ grows with the initial conditions of angles.

t_1 is defined as the first instant of time such that $\sqrt{\delta^2(t) + \epsilon^2(t)} \leq 0.07(rad)$ (or $4°$) for all $t > t_1$.

t_2 is defined as the time it taken to regulate well $\sqrt{x^2(t) + \ldots + \dot{\epsilon}^2(t)} \leq 0.15$ for all $t > t_2 \geq t_1$.

The angle variables are regulated fast as shown in Figure 7 even for large initial conditions of angles (δ, ϵ) where the slight fluctuation is due to disturbances. In this transient, translational dynamics are essentially not regulated. Therefore, an overshoot results in the $x - y$ plane. As seen in Figure 9, the overshoot in (x, y) becomes the more serious the larger the initial angles are. This leads to an increase in the time required to regulate to the origin (see Figure 8).

From the simulation results in Figures 3, 4, 5, one can observe that the closed loop system is robust

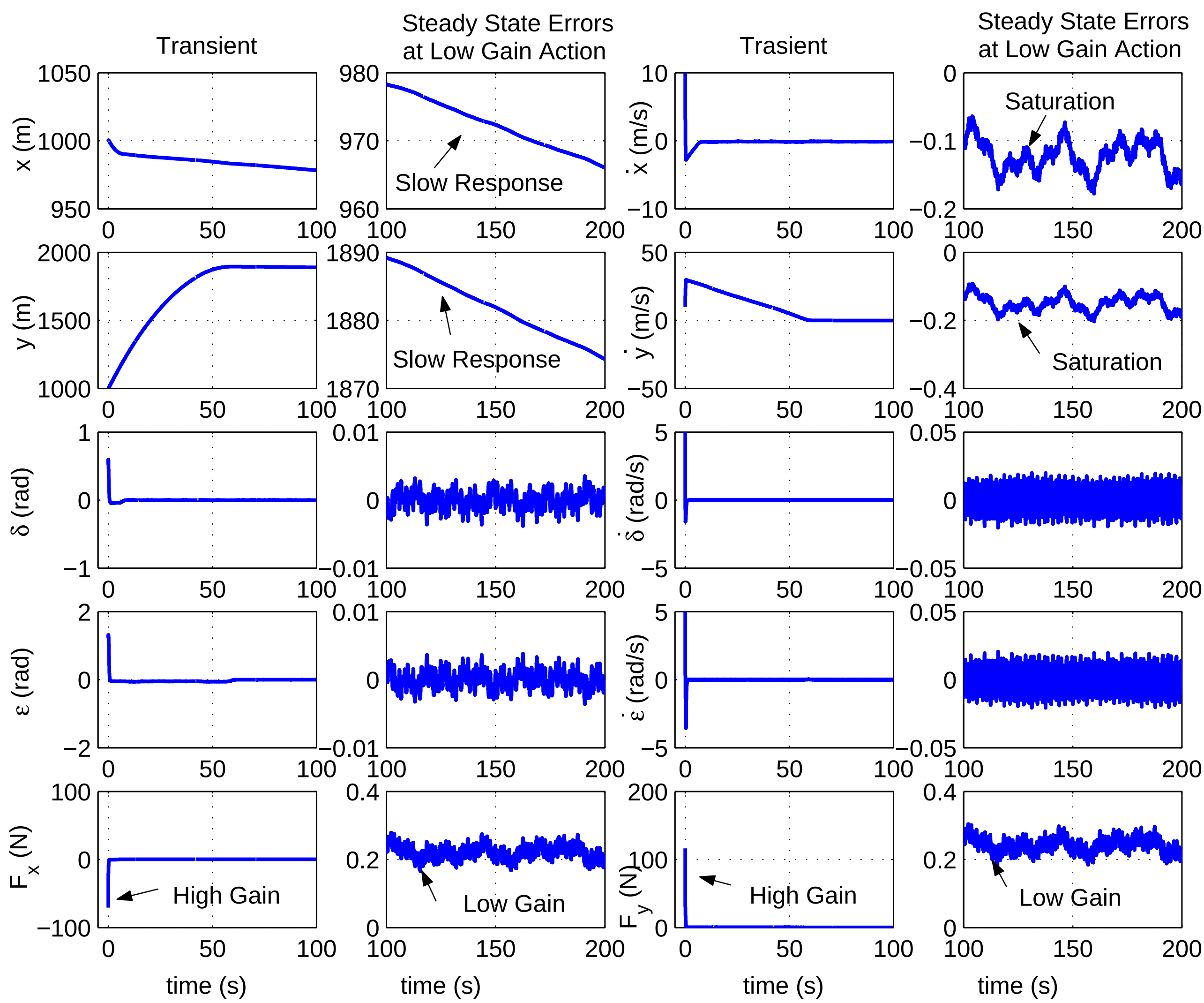

Figure 5. Simulation Results for *Case 3*

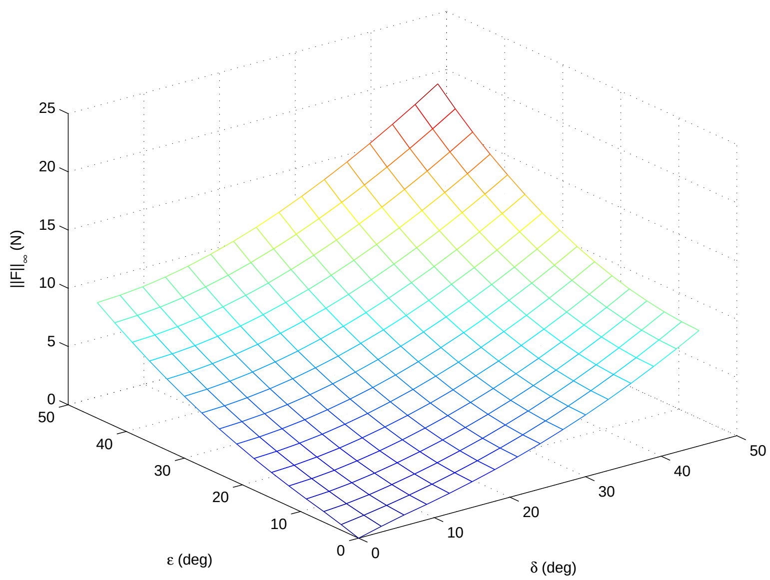

Figure 6. $\|F\|_\infty$ against the angles (δ, ϵ)

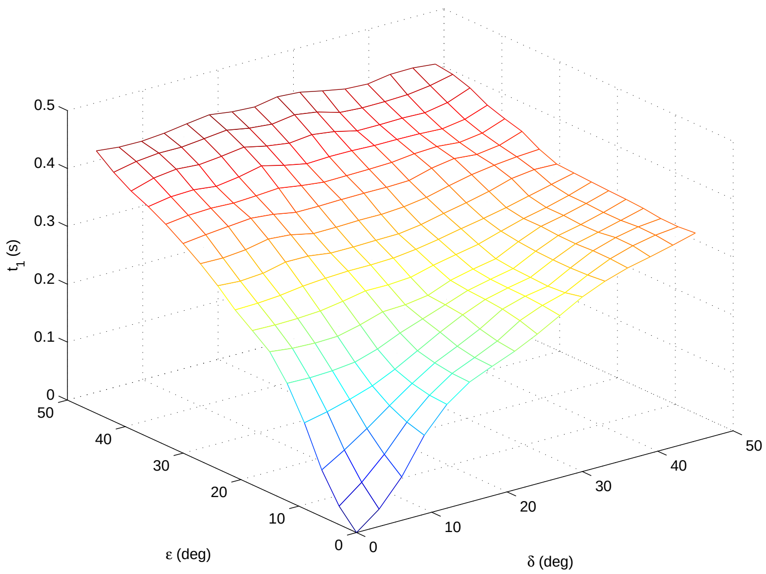

Figure 7. Time t_1 to the upright position against the angles (δ, ϵ)

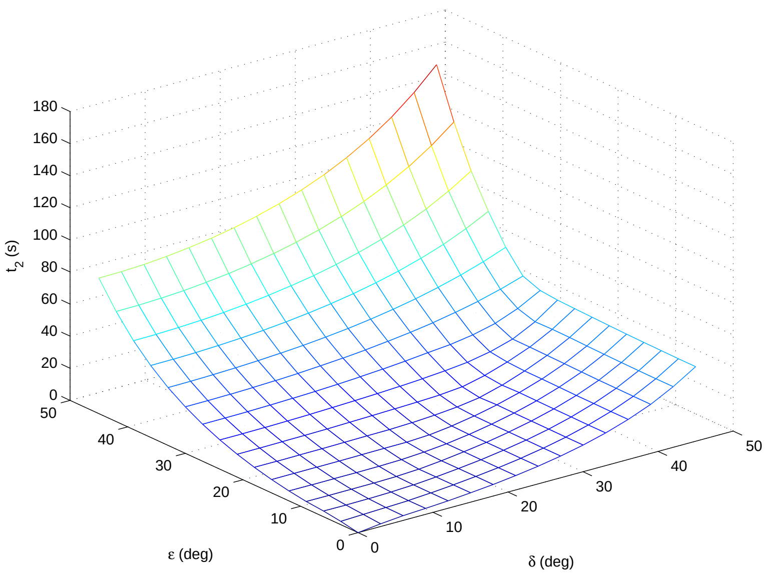

Figure 8. Time t_2 to the origin against the angles (δ, ϵ)

to small disturbances. To quantify the robustness through simulations, we consider the system under increasing magnitude exogenous disturbances Δ_{i2} for $i = 1, 2$ and compute the root mean square value of the position and angular responses. We define RMS for the position as

$$\mathrm{RMS}_{xy} \triangleq \sqrt{\frac{1}{T_0}\int_0^{T_0} x^2(t)dt + \frac{1}{T_0}\int_0^{T_0} y^2(t)dt} \tag{43}$$

and RMS for the angles

$$\mathrm{RMS}_{\delta\epsilon} \triangleq \sqrt{\frac{1}{T_0}\int_0^{T_0} \delta^2(t)dt + \frac{1}{T_0}\int_0^{T_0} \epsilon^2(t)dt}. \tag{44}$$

Figure 10 shows respectively the root mean square value of (x, y) response and the root mean square

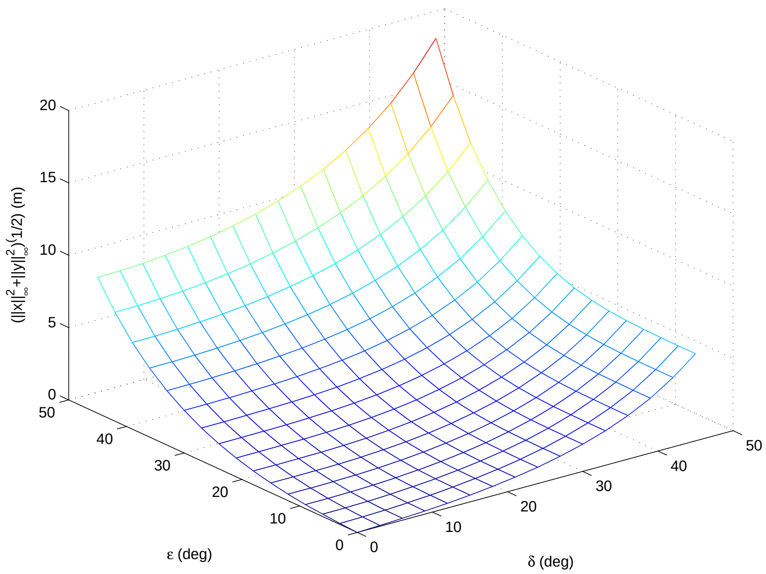

Figure 9. Overshoot $\sqrt{\|x\|_\infty^2 + \|y\|_\infty^2}$ against the angles (δ, ϵ)

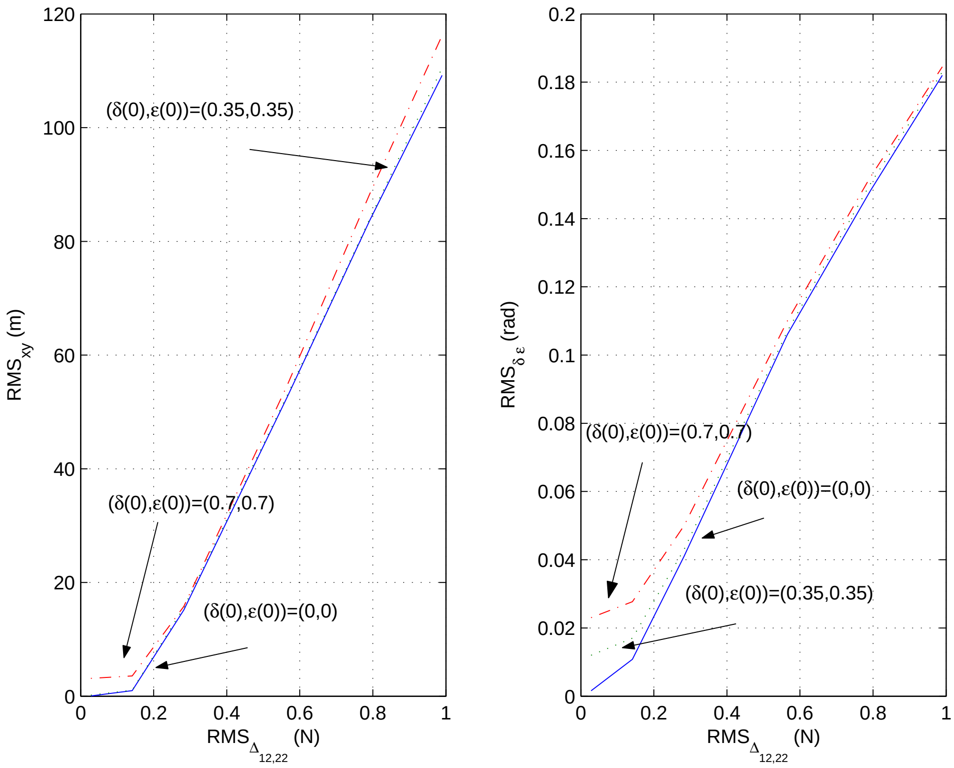

Figure 10. The impact of exogenous noises upon the performance

value of (δ, ϵ) response against the root mean square value of exogenous disturbance Δ_{12} (or Δ_{22}). When the disturbance intensity becomes too large, the trajectories of x and y wander off, but the trajectories of δ and ϵ remain tightly controlled around the upright position. Notice, as is to be expected, that the effect of the initial condition on the root mean square values is marginal due to the time averaging effect, and the fact that this effect is transitional only. The only reason why we see a dependence on the initial condition is because the root mean square value has been computed over a finite time window $t \in [0, T_0] = [0, 400](s)$.

5.3 *Summary of Simulation Studies*

We summarize the simulations with the following observations
1) the controller is reasonably robust with respect to unmodelled forces (see Figure 10);
2) the controller confirms the theory that the upright position has a large domain of attraction as shown in Figure 5 (see also Figure 10);
3) the overshoot problem becomes prominent when large initial conditions are given (see Figure 5);
4) the performance presents multi-scale separation in all cases;
5) there is no apparent time scale separation between x and y coordinates (respectively, $\dot{x}$ and $\dot{y}$) because the pendulum can be decoupled into two projections in $x-z$ plane and $y-z$ plane locally about the upper equilibrium.
6) the regulation of the angle variables is relatively fast (errors coupled via high gain control force).

6 Conclusion

We identified an appropriate upper triangular structure for the dynamics of the spherical inverted pendulum through appropriate coordinate and control transformations. The upper triangular structure we identified, allows us to design a controller using the forwarding methodology. The controller has a high and low gain structure. The errors in the angles are heavily penalized whilst the position errors are weakly penalized. The controller yields a large domain of attraction. Our simulation study confirms the theory and indicates that the controller enjoys a healthy level of robustness with respect to both unmodelled forces as well as unmodelled dynamics.

Acknowledgments

The authors would like to thank Dr. David Angeli who pointed out to the authors that forwarding maybe used for the spherical inverted pendulum. This research has been supported by the Centre of Excellence in Guidance and Control, funded by Defence Science & Technology Organization, Australia.

Appendix A: Entries of Equations (15)

The entries in the equations of dynamics (15) are listed as follows [1] the inertial matrix is

$$D(q) = m\begin{pmatrix} 1 & 0 & -Lc(\delta) & 0 \\ 0 & 1 & -Ls(\delta)s(\epsilon) & Lc(\epsilon)c(\delta) \\ -Lc(\delta) & -Ls(\delta)s(\epsilon) & L^2(1+1/3c(\epsilon)^2)+1/4R^2(1+s^2(\epsilon)) & 0 \\ 0 & Lc(\epsilon)c(\delta) & 0 & L^2(1/3+(c(\delta))^2)+1/4R^2 \end{pmatrix}$$

the Coriolis and centrifugal matrix is

$$C(q,\dot{q}) =$$
$$\begin{pmatrix} 0 & 0 & mL\dot{\delta}s(\delta) & 0 \\ 0 & 0 & -mL(\dot{\delta}s(\epsilon)c(\delta)+\dot{\epsilon}c(\epsilon)s(\delta)) & -mL(\dot{\epsilon}s(\epsilon)c(\delta)+\dot{\delta}c(\epsilon)s(\delta)) \\ 0 & 0 & (-1/3mL^2+1/4mR^2)\dot{\epsilon}c(\epsilon)s(\epsilon) & (-1/3mL^2+1/4mR^2)\dot{\delta}c(\epsilon)s(\epsilon)+mL^2\dot{\epsilon}c(\delta)s(\delta) \\ 0 & 0 & (1/3mL^2-1/4mR^2)\dot{\delta}c(\epsilon)s(\epsilon)-mL^2\dot{\epsilon}c(\delta)s(\delta) & -mL^2\dot{\delta}c(\delta)s(\delta) \end{pmatrix}$$

[1] To shorten the expression, $\sin(\cdot)$ is expressed as $s(\cdot)$ and $\cos(\cdot)$ is expressed as $c(\cdot)$.

the gravitational term is $G(q) = \big(0\,,0\,,-mgLs(\delta)c(\epsilon)\,,-mgLc(\delta)s(\epsilon)\big)$ and the generalized forces are $F_i = \big(F_x + v_{f_1}\,,F_y + v_{f_2}\,,v_{f_3}\,,v_{f_4}\big)$ with exogenous input $v_f = \big(v_{f_1}\,,v_{f_2}\,,v_{f_3}\,,v_{f_4}\big)$.

$[\dot{D}(q) - 2C(q,\dot{q})]$ is skew-symmetric as

$$[\dot{D}(q) - 2C(q,\dot{q})] = \begin{pmatrix} 0 & 0 & -mL\dot{\delta}s(\delta) & 0 \\ 0 & 0 & mL(\dot{\delta}s(\epsilon)c(\delta) + \dot{\epsilon}c(\epsilon)s(\delta)) & mL(\dot{\epsilon}s(\epsilon)c(\delta) + \dot{\delta}c(\epsilon)s(\delta)) \\ mL\dot{\delta}s(\delta) & -mL(\dot{\delta}s(\epsilon)c(\delta) + \dot{\epsilon}c(\epsilon)s(\delta)) & (1/3mL^2 - 1/4mR^2)\dot{\epsilon}c(\epsilon)s(\epsilon) & (1/3mL^2 - 1/4mR^2)\dot{\delta}c(\epsilon)s(\epsilon) - mL^2\dot{\epsilon}c(\delta)s(\delta) \\ 0 & -mL(\dot{\epsilon}s(\epsilon)c(\delta) + \dot{\delta}c(\epsilon)s(\delta)) & (1/4mR^2 - 1/3mL^2)\dot{\delta}c(\epsilon)s(\epsilon) + mL^2\dot{\epsilon}c(\delta)s(\delta) & mL^2\dot{\delta}c(\delta)s(\delta) \end{pmatrix}.$$

Appendix B: Entries of Equations (16)

$$\begin{aligned} \ddot{x} = {} & \frac{a(\delta,\epsilon)}{d(\delta,\epsilon)}\Big(F_x + v_{f_1} - mL\dot{\delta}^2 s(\delta)\Big) \\ & + \frac{j(\delta,\epsilon)}{d(\delta,\epsilon)}\Big(F_y + v_{f_2} + mL\dot{\delta}^2 s(\epsilon)c(\delta) + 2mL\dot{\delta}\dot{\epsilon}c(\epsilon)s(\delta) + mL\dot{\epsilon}^2 s(\epsilon)c(\delta)\Big) \\ & + \frac{Lc(\delta)e(\delta,\epsilon)}{d(\delta,\epsilon)}\Big(v_{f_3} + \dot{\epsilon}c(\epsilon)s(\epsilon)\dot{\delta}(2/3mL^2 - 1/2mR^2) - mL^2\dot{\epsilon}^2 c(\delta)s(\delta) + mgLs(\delta)c(\epsilon)\Big) \\ & + \frac{Lc(\delta)f(\delta,\epsilon)}{d(\delta,\epsilon)}\Big(v_{f_4} - \dot{\delta}^2 c(\epsilon)s(\epsilon)(1/3mL^2 - 1/4mR^2) + 2mL^2\dot{\delta}c(\delta)s(\delta)\dot{\epsilon} + mgLc(\delta)s(\epsilon)\Big) \end{aligned}$$

$$\begin{aligned} \ddot{y} = {} & \frac{j(\delta,\epsilon)}{d(\delta,\epsilon)}\Big(F_x + v_{f_1} - mL\dot{\delta}^2 s(\delta)\Big) \\ & + \frac{b(\delta,\epsilon)}{d(\delta,\epsilon)}\Big(F_y + v_{f_2} + mL\dot{\delta}^2 s(\epsilon)c(\delta) + 2mL\dot{\delta}\dot{\epsilon}c(\epsilon)s(\delta) + mL\dot{\epsilon}^2 s(\epsilon)c(\delta)\Big) \\ & + \frac{g(\delta,\epsilon)}{d(\delta,\epsilon)}\Big(v_{f_3} + \dot{\epsilon}c(\epsilon)s(\epsilon)\dot{\delta}(2/3mL^2 - 1/2mR^2) - mL^2\dot{\epsilon}^2 c(\delta)s(\delta) + mgLs(\delta)c(\epsilon)\Big) \\ & + \frac{h(\delta,\epsilon)}{d(\delta,\epsilon)}\Big(v_{f_4} - \dot{\delta}^2 c(\epsilon)s(\epsilon)(1/3mL^2 - 1/4mR^2) + 2mL^2\dot{\delta}c(\delta)s(\delta)\dot{\epsilon} + mgLc(\delta)s(\epsilon)\Big) \end{aligned}$$

$$\begin{aligned} \ddot{\delta} = {} & \frac{Lc(\delta)e(\delta,\epsilon)}{d(\delta,\epsilon)}\Big(F_x + v_{f_1} - mL\dot{\delta}^2 s(\delta)\Big) \\ & + \frac{g(\delta,\epsilon)}{d(\delta,\epsilon)}\Big(F_y + v_{f_2} + mL\dot{\delta}^2 s(\epsilon)c(\delta) + 2mL\dot{\delta}\dot{\epsilon}c(\epsilon)s(\delta) + mL\dot{\epsilon}^2 s(\epsilon)c(\delta)\Big) \\ & + \frac{e(\delta,\epsilon)}{d(\delta,\epsilon)}\Big(v_{f_3} + \dot{\epsilon}c(\epsilon)s(\epsilon)\dot{\delta}(2/3mL^2 - 1/2mR^2) - mL^2\dot{\epsilon}^2 c(\delta)s(\delta) + mgLs(\delta)c(\epsilon)\Big) \\ & + \frac{f(\delta,\epsilon)}{d(\delta,\epsilon)}\Big(v_{f_4} - \dot{\delta}^2 c(\epsilon)s(\epsilon)(1/3mL^2 - 1/4mR^2) + 2mL^2\dot{\delta}c(\delta)s(\delta)\dot{\epsilon} + mgLc(\delta)s(\epsilon)\Big) \end{aligned}$$

$$
\begin{aligned}
\ddot{\epsilon} = & \frac{Lc(\delta)f(\delta,\epsilon)}{d(\delta,\epsilon)}\left(F_x + v_{f_1} - mL\dot{\delta}^2 s(\delta)\right) \\
& + \frac{h(\delta,\epsilon)}{d(\delta,\epsilon)}\left(F_y + v_{f_2} + mL\dot{\delta}^2 s(\epsilon)c(\delta) + 2mL\dot{\delta}\dot{\epsilon}c(\epsilon)s(\delta) + mL\dot{\epsilon}^2 s(\epsilon)c(\delta)\right) \\
& + \frac{f(\delta,\epsilon)}{d(\delta,\epsilon)}\left(v_{f_3} + \dot{\epsilon}c(\epsilon)s(\epsilon)\dot{\delta}(2/3mL^2 - 1/2mR^2) - mL^2\dot{\epsilon}^2 c(\delta)s(\delta) + mgLs(\delta)c(\epsilon)\right) \\
& + \frac{i(\delta,\epsilon)}{d(\delta,\epsilon)}\left(v_{f_4} - \dot{\delta}^2 c(\epsilon)s(\epsilon)(1/3mL^2 - 1/4mR^2) + 2mL^2\dot{\delta}c(\delta)s(\delta)\dot{\epsilon} + mgLc(\delta)s(\epsilon)\right)
\end{aligned}
$$

where

$$
\begin{aligned}
a(\delta,\epsilon) = & -108R^2L^2(c(\delta))^2 + 9R^4(c(\epsilon))^2 - 36L^2(c(\epsilon))^2R^2 - 48L^4(c(\delta))^2 + 48L^4(c(\epsilon))^4(c(\delta))^2 \\
& -64L^4(c(\epsilon))^2 - 144(c(\delta))^4L^4 + 144L^2(c(\epsilon))^2(c(\delta))^2R^2 + 144(c(\delta))^4L^4(c(\epsilon))^2 - \\
& 36L^2(c(\epsilon))^4(c(\delta))^2R^2 - 24L^2R^2 - 18R^4;
\end{aligned}
$$

$$
\begin{aligned}
b(\delta,\epsilon) = & -(48L^4 + 96L^4(c(\delta))^2 + 60L^2R^2 + 16L^4(c(\epsilon))^2 + 48L^4(c(\epsilon))^2(c(\delta))^2 + \\
& 18R^4 + 36R^2L^2(c(\delta))^2 - 36L^2(c(\epsilon))^2(c(\delta))^2R^2 - 9R^4(c(\epsilon))^2 - 144(c(\delta))^4L^4)
\end{aligned}
$$

$$
j(\delta,\epsilon) = -12L^2c(\delta)s(\delta)s(\epsilon)(4L^2 + 12L^2(c(\delta))^2 + 3R^2)
$$

$$
\begin{aligned}
d(\delta,\epsilon) = & m(-72R^2L^2(c(\delta))^2 + 9R^4(c(\epsilon))^2 - 36L^2(c(\epsilon))^2R^2 + 48L^4(c(\epsilon))^4(c(\delta))^2 \\
& -64L^4(c(\epsilon))^2 + 144L^2(c(\epsilon))^2(c(\delta))^2R^2 - 36L^2(c(\epsilon))^4(c(\delta))^2R^2 - 24L^2R^2 - 18R^4)
\end{aligned}
$$

$$
e(\delta,\epsilon) = 12(-4L^2 - 12L^2(c(\delta))^2 - 3R^2 + 12(c(\epsilon))^2(c(\delta))^2L^2)
$$

$$
f(\delta,\epsilon) = 144L^2c(\delta)s(\delta)s(\epsilon)c(\epsilon)
$$

$$
g(\delta,\epsilon) = -12Ls(\delta)s(\epsilon)(4L^2 + 12L^2(c(\delta))^2 + 3R^2)
$$

$$
h(\delta,\epsilon) = 12Lc(\epsilon)c(\delta)(12L^2 + 4L^2(c(\epsilon))^2 + 6R^2 - 3(c(\epsilon))^2R^2 - 12L^2(c(\delta))^2)
$$

$$
i(\delta,\epsilon) = 12(-16L^2(c(\epsilon))^2 - 6R^2 + 3(c(\epsilon))^2R^2 + 12(c(\epsilon))^2(c(\delta))^2L^2)\,.
$$

Appendix C: Entries of $H_{11}(\delta,\epsilon)$, $H_{12}(\delta,\epsilon)$, $H_{21}(\delta,\dot{\delta},\epsilon,\dot{\epsilon})$, $H_{22}(\delta,\dot{\delta},\epsilon,\dot{\epsilon})$

Let the radius $R = 0$ and the exogenous input $v_f = 0$ in the design. In this case,

$$
a(\delta,\epsilon) = -48L^4(c(\delta))^2 + 48L^4(c(\epsilon))^4(c(\delta))^2 - 64L^4(c(\epsilon))^2 - 144(c(\delta))^4L^4 + 144(c(\delta))^4L^4(c(\epsilon))^2
$$

$$b(\delta,\epsilon) = -(48L^4 + 96L^4(c(\delta))^2 + 16L^4(c(\epsilon))^2 + 48L^4(c(\epsilon))^2(c(\delta))^2 - 144(c(\delta))^4L^4)$$

$$d(\delta,\epsilon) = -16mL^4(c(\epsilon))^2(4 - 3(c(\epsilon))^2(c(\delta))^2)$$

$$j(\delta,\epsilon) = -12L^2c(\delta)s(\delta)s(\epsilon)(4L^2 + 12L^2(c(\delta))^2)$$

$$e(\delta,\epsilon) = 12(-4L^2 - 12L^2(c(\delta))^2 + 12(c(\epsilon))^2(c(\delta))^2L^2)$$

$$f(\delta,\epsilon) = 144L^2c(\delta)s(\delta)s(\epsilon)c(\epsilon)$$

$$g(\delta,\epsilon) = -12Ls(\delta)s(\epsilon)(4L^2 + 12L^2(c(\delta))^2)$$

$$h(\delta,\epsilon) = 12Lc(\epsilon)c(\delta)(12L^2 + 4L^2(c(\epsilon))^2 - 12L^2(c(\delta))^2)$$

$$i(\delta,\epsilon) = 12(-16L^2(c(\epsilon))^2 + 12(c(\epsilon))^2(c(\delta))^2L^2)\,.$$

Since $d(\delta,\epsilon) = -16mL^4(c(\epsilon))^2(4 - 3(c(\epsilon))^2(c(\delta))^2) < 0$ holds for any $(\delta,\epsilon) \in \left(-\frac{\pi}{2}, -\frac{\pi}{2}\right)$, $H_{11}(\delta,\epsilon)$, $H_{12}(\delta,\epsilon)$, $H_{21}(\delta,\dot{\delta},\epsilon,\dot{\epsilon})$, $H_{22}(\delta,\dot{\delta},\epsilon,\dot{\epsilon})$ are valid on U as are defined next.

$$H_{11}(\delta,\epsilon) = \begin{pmatrix} \frac{a(\delta,\epsilon)}{d(\delta,\epsilon)} & \frac{j(\delta,\epsilon)}{d(\delta,\epsilon)} \\ \\ \frac{j(\delta,\epsilon)}{d(\delta,\epsilon)} & \frac{b(\delta,\epsilon)}{d(\delta,\epsilon)} \end{pmatrix}, \; H_{21}(\delta,\epsilon) = \begin{pmatrix} \frac{Lc(\delta)e(\delta,\epsilon)}{d(\delta,\epsilon)} & \frac{g(\delta,\epsilon)}{d(\delta,\epsilon)} \\ \\ \frac{Lc(\delta)f(\delta,\epsilon)}{d(\delta,\epsilon)} & \frac{h(\delta,\epsilon)}{d(\delta,\epsilon)} \end{pmatrix}$$

Because $\det(H_{21}(\delta,\epsilon)) = -\frac{Lc(\delta)}{(d(\delta,\epsilon))^2}\left(2304L^5(c(\epsilon))^3c(\delta)\left(4 - 3(c(\epsilon))^2(c(\delta))^2\right)\right) < 0$ hold for any $(\delta,\epsilon) \in U$, $H_{21}(\delta,\epsilon)$ is invertible on U.

$$H_{12}(\delta,\dot{\delta},\epsilon,\dot{\epsilon}) = \begin{pmatrix} \frac{a(\delta,\epsilon)}{d(\delta,\epsilon)}\left(-mL\dot{\delta}^2s(\delta)\right) \\ +\frac{j(\delta,\epsilon)}{d(\delta,\epsilon)}\left(mL\dot{\delta}^2s(\epsilon)c(\delta) + 2mL\dot{\delta}\dot{\epsilon}c(\epsilon)s(\delta) + mL\dot{\epsilon}^2s(\epsilon)c(\delta)\right) \\ +\frac{Lc(\delta)e(\delta,\epsilon)}{d(\delta,\epsilon)}\left(\dot{\epsilon}c(\epsilon)s(\epsilon)\dot{\delta}2/3mL^2 - mL^2\dot{\epsilon}^2c(\delta)s(\delta) + mgLs(\delta)c(\epsilon)\right) \\ +\frac{Lc(\delta)f(\delta,\epsilon)}{d(\delta,\epsilon)}\left(-\dot{\delta}^2c(\epsilon)s(\epsilon)1/3mL^2 + 2mL^2\dot{\delta}c(\delta)s(\delta)\dot{\epsilon} + mgLc(\delta)s(\epsilon)\right) \\ \hline \frac{j(\delta,\epsilon)}{d(\delta,\epsilon)}\left(-mL\dot{\delta}^2s(\delta)\right) \\ +\frac{b(\delta,\epsilon)}{d(\delta,\epsilon)}\left(mL\dot{\delta}^2s(\epsilon)c(\delta) + 2mL\dot{\delta}\dot{\epsilon}c(\epsilon)s(\delta) + mL\dot{\epsilon}^2s(\epsilon)c(\delta)\right) \\ +\frac{g(\delta,\epsilon)}{d(\delta,\epsilon)}\left(\dot{\epsilon}c(\epsilon)s(\epsilon)\dot{\delta}2/3mL^2 - mL^2\dot{\epsilon}^2c(\delta)s(\delta) + mgLs(\delta)c(\epsilon)\right) \\ +\frac{h(\delta,\epsilon)}{d(\delta,\epsilon)}\left(-\dot{\delta}^2c(\epsilon)s(\epsilon)1/3mL^2 + 2mL^2\dot{\delta}c(\delta)s(\delta)\dot{\epsilon} + mgLc(\delta)s(\epsilon)\right) \end{pmatrix}$$

$$H_{22}(\delta,\dot{\delta},\epsilon,\dot{\epsilon}) = \left(\frac{\begin{array}{c}\frac{Lc(\delta)e(\delta,\epsilon)}{d(\delta,\epsilon)}\left(-mL\dot{\delta}^2 s(\delta)\right)\\ +\frac{g(\delta,\epsilon)}{d(\delta,\epsilon)}\left(mL\dot{\delta}^2 s(\epsilon)c(\delta)+2mL\dot{\delta}\dot{\epsilon}c(\epsilon)s(\delta)+mL\dot{\epsilon}^2 s(\epsilon)c(\delta)\right)\\ +\frac{e(\delta,\epsilon)}{d(\delta,\epsilon)}\left(\dot{\epsilon}c(\epsilon)s(\epsilon)\dot{\delta}2/3mL^2-mL^2\dot{\epsilon}^2c(\delta)s(\delta)+mgLs(\delta)c(\epsilon)\right)\\ +\frac{f(\delta,\epsilon)}{d(\delta,\epsilon)}\left(-\dot{\delta}^2c(\epsilon)s(\epsilon)1/3mL^2+2mL^2\dot{\delta}c(\delta)s(\delta)\dot{\epsilon}+mgLc(\delta)s(\epsilon)\right)\end{array}}{\begin{array}{c}\frac{Lc(\delta)f(\delta,\epsilon)}{d(\delta,\epsilon)}\left(-mL\dot{\delta}^2 s(\delta)\right)\\ +\frac{h(\delta,\epsilon)}{d(\delta,\epsilon)}\left(mL\dot{\delta}^2 s(\epsilon)c(\delta)+2mL\dot{\delta}\dot{\epsilon}c(\epsilon)s(\delta)+mL\dot{\epsilon}^2 s(\epsilon)c(\delta)\right)\\ +\frac{f(\delta,\epsilon)}{d(\delta,\epsilon)}\left(\dot{\epsilon}c(\epsilon)s(\epsilon)\dot{\delta}2/3mL^2-mL^2\dot{\epsilon}^2c(\delta)s(\delta)+mgLs(\delta)c(\epsilon)\right)\\ +\frac{i(\delta,\epsilon)}{d(\delta,\epsilon)}\left(-\dot{\delta}^2c(\epsilon)s(\epsilon)1/3mL^2+2mL^2\dot{\delta}c(\delta)s(\delta)\dot{\epsilon}+mgLc(\delta)s(\epsilon)\right)\end{array}}\right)$$

Appendix D: Details of Design Step 3-6

Details of Design Step 3

$$F_2 = \left[\frac{\partial f_2(\xi_2,\alpha_1(\xi_1,v_1))}{\partial \xi_2}\right]_{(0,0)} = \begin{pmatrix} 0 & 0 & 0 & 49.83 & 8.01 \\ 0 & 0 & 1 & 0 & 0 \\ 0 & -100 & -20 & 0 & 0 \\ 0 & 0 & 0 & 0 & 1 \\ 0 & 0 & 0 & -100 & -20 \end{pmatrix},$$

$$G_2 = \left[\frac{\partial f_2(\xi_2,\alpha_1(\xi_1,v_1))}{\partial v_1}\right]_{(0,0)} = \begin{pmatrix} 0 & 11.4 \\ 0 & 0 \\ 28.5 & 0 \\ 0 & 0 \\ 0 & -28.5 \end{pmatrix}.$$

Assigning $Q = diag(100, 100, 20, 100, 20)$ and $R = diag(0.5, 0.5)$ obtains

$$K_2 = \begin{pmatrix} 0 & -11.06 & -5.72 & 0 & 0 \\ 14.1 & 0 & 0 & 61.4 & 13.7 \end{pmatrix}.$$

All eigenvalues of $(F_2 + G_2K_2)$ are in C^-.

Details of Design Step 4

$$F_3 = \left[\frac{\partial f_3(\xi_3,\alpha_2(\xi_2,v_2))}{\partial \xi_3}\right]_{(0,0)} = \begin{pmatrix} 0 & 0 & -175.9 & -73.24 & 0 & 0 \\ 0 & 161.2 & 0 & 0 & 749.9 & 164.5 \\ 0 & 0 & 0 & 1 & 0 & 0 \\ 0 & 0 & -415.0 & -183.9 & 0 & 0 \\ 0 & 0 & 0 & 0 & 0 & 1 \\ 0 & -402.8 & 0 & 0 & -1848 & -410.8 \end{pmatrix},$$

$$G_3 = \left[\frac{\partial f_3(\xi_3, \alpha_2(\xi_2, v_2))}{\partial v_2}\right]_{(0,0)} = \begin{pmatrix} 11.4 & 0 \\ 0 & 11.4 \\ 0 & 0 \\ 28.5 & 0 \\ 0 & 0 \\ 0 & -28.5 \end{pmatrix}.$$

Assigning $Q = diag(100, 100, 100, 20, 100, 20)$ and $R = diag(0.5, 0.5)$ obtains

$$K_3 = \begin{pmatrix} 14.1 & 0 & -55.9 & -10.06 & 0 & 0 \\ 0 & 5.71 & 0 & 0 & 26.5 & 5.80 \end{pmatrix}.$$

All eigenvalues of $(F_3 + G_3K_3)$ are in C^-.

Details of Design Step 5

$$F_4 = \left[\frac{\partial f_4(\xi_4, \alpha_3(\xi_3, v_3))}{\partial \xi_4}\right]_{(0,0)} = \begin{pmatrix} 0 & 0 & 1 & 0 & 0 & 0 & 0 \\ 0 & 161.2 & 0 & -813.9 & -188.0 & 0 & 0 \\ 0 & 0 & 226.3 & 0 & 0 & 1052 & 230.6 \\ 0 & 0 & 0 & 0 & 1 & 0 & 0 \\ 0 & 402.8 & 0 & -2008 & -469.6 & 0 & 0 \\ 0 & 0 & 0 & 0 & 0 & 0 & 1 \\ 0 & 0 & -565.4 & 0 & 0 & -2604 & -576 \end{pmatrix},$$

$$G_4 = \left[\frac{\partial f_4(\xi_4, \alpha_3(\xi_3, v_3))}{\partial v_3}\right]_{(0,0)} = \begin{pmatrix} 0 & 0 \\ 11.4 & 0 \\ 0 & 11.4 \\ 0 & 0 \\ 28.5 & 0 \\ 0 & 0 \\ 0 & -28.5 \end{pmatrix}.$$

Assigning $Q = diag(100, 100, 100, 100, 20, 100, 20)$ and $R = diag(0.5, 0.5)$ obtains

$$K_4 = \begin{pmatrix} 0 & 5.71 & 0 & -24.61 & -5.28 & 0 & 0 \\ 14.14 & 0 & 10.85 & 0 & 0 & 34.1 & 7.06 \end{pmatrix}.$$

All eigenvalues of $(F_4 + G_4K_4)$ are in C^-.

Details of Design Step 6

$$F_5 = \left[\frac{\partial f_5(\xi_5, \alpha_4(\xi_4, v_4))}{\partial \xi_5}\right]_{(0,0)} = \begin{pmatrix} 0 & 0 & 1 & 0 & 0 & 0 & 0 & 0 \\ 0 & 0 & 0 & 1 & 0 & 0 & 0 & 0 \\ 0 & 0 & 226.2 & 0 & -1094 & -248.2 & 0 & 0 \\ 0 & 161.2 & 0 & 350 & 0 & 0 & 1441 & 311.1 \\ 0 & 0 & 0 & 0 & 0 & 1 & 0 & 0 \\ 0 & 0 & 565.3 & 0 & -2709 & -619.9 & 0 & 0 \\ 0 & -402.8 & 0 & 0 & 0 & 0 & 0 & 1 \\ 0 & 0 & 0 & -874.4 & 0 & 0 & -3575 & -777 \end{pmatrix},$$

$$G_5 = \left[\frac{\partial f_5(\xi_5, \alpha_4(\xi_4, v_4))}{\partial v_4}\right]_{(0,0)} = \begin{pmatrix} 0 & 0 \\ 0 & 0 \\ 11.4 & 0 \\ 0 & 11.4 \\ 0 & 0 \\ 28.5 & 0 \\ 0 & 0 \\ 0 & -28.5 \end{pmatrix}.$$

Assigning $Q = diag(100, 100, 100, 100, 100, 20, 100, 20)$ and $R = diag(0.5, 0.5)$ obtains

$$K_5 = \begin{pmatrix} 14.1 & 0 & 4.87 & 0 & -29.5 & -8.75 & 0 & 0 \\ 0 & 5.62 & 0 & 6.97 & 0 & 0 & 34.3 & 9.23 \end{pmatrix}.$$

All eigenvalues of $(F_5 + G_5K_5)$ are in C^-.

References

X. Albouy and L. Praly, "On the use of dynamic invariants and forwarding for swinging up a spherical inverted pendulum," in *Proc. of 39th Conference on Decision & Control*, Sydney, Australia,, 2000, pp. 1667–1672.

R. Yang, Y. Kuen, and Z. Li, "Stabilisation of a 2-dof spherical pendulum on x-y table," in *Proc. of the 2000 IEEE international conference on control application*, Anchorage, Alaska, USA, 2000, pp. 724–729.

C. Chung, J. Lee, S. Lee, and B. Lee, "Balancing of an inverted pendulum with a redundant direct-drive robot," in *Proc. of the 2000 IEEE international conference on robotics & automation*, San Francisco, CA, USA, 2000, pp. 3952–3957.

A. Bloch, N. Leonard, and J. Marsden, "Controlled lagragians and the stabilisation of mechanical systems i:the first matching theorem," *IEEE Transaction on Automatic Control*, vol. 45, pp. 2253–2269, 2000.

A. Bloch, D. Chang, N. Leonard, and J. Marsden, "Controlled lagragians and the stabilisation of mechanical systems ii: potential shaping," *IEEE Transaction on Automatic Control*, vol. 46, pp. 1556–1571, 2001.

D. Angeli, "Global stabilisation of the inverted pendulum via continuous state feedback," 2001, a report.

——, "Almost global stabilisation of the inverted pendulum via continuous state feedback," *Automatica*, vol. 37, pp. 1103–1108, 2001.

A. Teel, "A nonlinear small gain theorem for the analysis of control systems with saturation," *IEEE Transactions on Automatic Control*, vol. 41, pp. 1256–1270, 1996.

G. Liu, D. Nešić, and I. Mareels, "Modelling and stabilisation of a spherical inverted pendulum," in *Proceeding of IFAC*, 2005.

A. Isidori, *Nonlinear Control System II.* Springer, 1999.

E. Sontag, “Smooth stabilization implies comprime factorization,” *IEEE Transaction on Automatic Control*, vol. 35, pp. 435–443, 1989.

——, “Further facts about input to state stabilization,” *IEEE Transactions on Automatic Control*, vol. 35, pp. 473–476, 1990.

E. Sontag and Y. Wang, “On characterizations of the input-to-state stability property,” *Systems and Control Letters*, vol. 24, pp. 351–359, 1995.

J. Slotine and W. Li, *Applied Nonlinear Control*. Prentice Hall, 1991.

N. Hand, *Analytical mechanics*. Cambridge: Cambridge University Press, 1998.

F. Mazenc and L. Praly, “Adding integrations, saturated controls, and stabilization for feedforward systems,” *IEEE Transactions on Automatic Control*, vol. 41, pp. 1559–1577, 1996.

R. Olfati-Saber “Nonlinear Control of Underactuated Mechanical Systems with Application to Robotics and Aerospace Vehicles,” *Ph.D Thesis, Massachusetts Institute of Technology*, 2001.